New data on the chronology of the Vale do Forno sedimentary sequence (Lower Tejo River terrace staircase) and its relevance as a fluvial archive of the Middle Pleistocene in western Iberia

Cunha, Pedro; Martins, Antonio; Buylaert, Jan-Pieter; Murray, Andrew Sean; Raposo, Luis; Mozzi, Paolo; Stokes, Martin

Published in:
Quaternary Science Reviews

Link to article, DOI:
10.1016/j.quascirev.2016.11.001

Publication date:
2017

Document Version
Peer reviewed version

QSR ; Article Type: Special Issue - Fluvial Archives Group

JQSR-16-00187-Manuscript_rev1

New data on the chronology of the Vale do Forno sedimentary sequence (Lower Tejo River terrace staircase) and its relevance as a fluvial archive of the Middle Pleistocene in western Iberia

Pedro P. Cunha [a *], António A. Martins [b], Jan-Pieter Buylaert [c,d], Andrew S. Murray [d], Luis Raposo [e], Paolo Mozzi [f], Martin Stokes [g]

[a] MARE - Marine and Environmental Sciences Centre, Department of Earth Sciences, Universidade de Coimbra, Rua Sílvio Lima, Univ. Coimbra - Pólo II; 3030-790 Coimbra, Portugal: pcunha@dct.uc.pt
[b] Instituto de Ciências da Terra (ICT), Departamento de Geociências, Universidade de Évora, Colégio Luís António Verney, Rua Romão Ramalho, 59, 7000-671 Évora, Portugal; aam@uevora.pt
c Centre for Nuclear Technologies, Technical University of Denmark, Risø Campus, Denmark; jabu@dtu.dk
d Nordic Laboratory for Luminescence Dating, Aarhus University, Risø DTU, Denmark; anmu@dtu.dk
e Museu Nacional de Arqueologia, Praça do Império. 1400-206 Lisboa, Portugal; 3raposos@sapo.pt
f Department of Geosciences, University of Padova, 35121 Padova, Italy; paolo.mozzi@unipd.it
g School of Geography, Earth and Environmental Sciences, University of Plymouth, Plymouth, Devon PL4 8AA, UK; m.stokes@plymouth.ac.uk

ABSTRACT

The Vale do Forno archaeological sites (Alpiarça, central Portugal) document the earliest human occupation in the Lower Tejo River, well established in geomorphological and environmental terms, within the Middle Pleistocene. In a staircase of six fluvial terraces, the Palaeolithic sites were found on the T4 terrace (+24 m, above river bed) which is made of a basal Lower Gravels unit (LG) and an overlying Upper Sands unit (US). Geomorphological mapping, coupled with lithostratigraphy, sedimentology and luminescence dating (quartz-OSL and K-feldspar post-IRIR_{290}) were used in this study. The oldest artefacts found in the LG unit show crude bifacial forms that can be attributed

* Corresponding author. E-mail address: pcunha@dct.uc.pt. Departamento de Ciências da Terra, Universidade de Coimbra, Rua Sílvio Lima, Univ. Coimbra - Pólo II; 3030-790 Coimbra, Portugal. Tel. +351 239860541, Fax. +351 239860501

to the Acheulian. In contrast, the US unit has archaeological sites stratigraphically documenting successive phases of an evolved Acheulian. Luminescence dating and correlation with the Marine Isotopic Stages suggest that the LG unit has a probable age of ca. 335 to 325 ka and the US unit an age of ca. 325 to 155 ka. This is in contrast to previous interpretations ascribing this terrace (and lithic industries) to the Last Interglacial and early phases of the Last Glacial. The VF3 site (Milharós), containing Micoquian (Final Acheulian) industries (with fine and elaborated bifaces), found in a stratigraphic level located between the T4 terrace deposits and a colluvium associated with Late Pleistocene aeolian sands, is younger than 155 ka but much older than 32 ka.

Keywords: Palaeolithic; Acheulean; Middle Pleistocene; geomorphology; luminescence dating; fluvial terraces; River Tejo; Iberia.

1. Introduction

Understanding of the Palaeolithic occupation of Northern Europe has been substantially based on evidence from rivers (e.g. Bridgland et al., 2006). For Western Europe and specifically in Iberia, insights into the Palaeolithic occupation is similarly derived from its major rivers (from north to south: Douro, Tejo/Tagus, Guadiana, Guadalquivir) (e.g. Santoja and Villa, 2006). Within this context, the Vale do Forno archaeological sites (Alpiarça, in central Portugal; Fig. 1) provide the earliest and most well documented human occupation in the Lower Tejo (the Portuguese part of the Tejo basin). Lower Palaeolithic bifacial sites are common, often well represented by lithic industries. Their local stratigraphy and technological characteristics indicate successive phases of what is commonly named as the Acheulian. However, they were chronologically poorly constrained.

From the Spanish border to the Atlantic coast, the Tejo crosses major faults which provide a natural geomorphological subdivision of the river into a series of valley reaches (I to V; Cunha et al., 2005). In Reach I, within the Ródão and Arneiro depressions, the Tejo has cut well-developed staircases of alluvial terraces (Cunha et al., 2008, 2012), built on a sedimentary bedrock of the Lower Tejo Cenozoic Basin (LTCB; e.g. Pais et al., 2012). Here, the Tejo also flows across a series of highly resistant quartzite ridges. In Reach II, the Tejo flows over Paleozoic basement through a NE–SW orientated valley for some 30 km along which terraces are largely absent. In reach III, the Tejo is routed E–W, crossing three structural depressions with a Tertiary cover (Martins et al., 2009). In reach IV, the Tejo changes to a NNE–SSW trend, with valley sides displaying different degrees of terrace staircase development (Martins et al., 2010a, 2010b) (Figs. 1 and 2). Reach V corresponds to the Tejo estuary which covers a wide area but its final connection to the Atlantic is through a gorge. Here, terraces are not well described. Throughout the Lower Tejo region the best developed terraces, sometimes forming up to six levels, are typically associated with areas of weaker bedrock (e.g. Tertiary sediments in Reaches I, II and IV) where the river has been able to enlarge the valley.

The study area is located on the left flank of the middle part of a ~85 km long NNE-SSW orientated valley-section of reach IV, some ~100 km from the river mouth. The geomorphological characteristics of this reach are quite different from the Lower Tejo upstream (reaches I, II and III). In reach IV, the Tejo has a wide alluvial plain (up to 10 km wide) with an extensive staircase of six fluvial terraces (T1 to T6) developed along its valley sides (Martins, 1999). Here, the modern Tejo can be considered a low sinuosity, single-channel river with large sand bars, and its alluvial plain connects with a tide-dominated estuary.

The NNE-SSW oriented valley of reach IV is controlled by the NNE-SSW Lower Tejo Valley fault zone (e.g. Choffat, 1907; Bensaúde, 1910; Freire de Andrade, 1933; Cabral *et al.* 2003, 2004, 2013; Cabral and Ribeiro, 1988, 1989; Cabral, 1995, 2012; Vilanova and Fonseca, 2004; Carvalho et al., 2008, 2014; Martins et al. 2009; Besana-Ostman et al. 2012). This is expressed as a regional scale tectonic lineament concealed by Holocene sediments. This valley is developed in a low uplift area (<100 m during the last ca. 2 Ma) with some subsidence in the present estuary (reach V). The interplay between these regional tectonic characteristics and Pleistocene to Holocene glacio-eustatic sea-level changes has strongly influenced the formation of fluvial terraces and sedimentary valley-fill (eg. Merritts et al., 1994; Blum and Törnqvist, 2000). The high amplitude sea-level changes that characterized the Middle and Late Pleistocene controlled the episodic down-cutting phases of the river during sea-level lowstands; these alternated with flooding and agradation phases in the incised valley during highstands (Cunha et al., 2016). Such climate related eustatic oscillations are superimposed on a long-term uplift pattern, both phenomena having controlled the river terrace staircase development (Cunha et al., 2005, 2008; Martins et al., 2010a, 2010b).

In reach IV, several archaeological studies have been undertaken in the last 70 years (e.g. Breuil and Zbyszewsky, 1942, 1945; Zbyszewski, 1946; Raposo, 1995a, 1995b; Mozzi et al., 2000). The prehistoric human occupation of this area is of renewed interest because it contains evidence for an extensive Palaeolithic occupation. Related archaeological sites are present on both sides of the river, from the Lisboa area to the vicinity of Torres Novas (Fig. 2). The site of Santo Antão do Tojal (near the estuary) is considered especially important, because dated fossil remains of *Palaeoloxodon antiquus* and *Equus caballus* were found in association with lithic industries (Zbyszewski, 1943,

1977; Raposo, 1995a). The study of these sites has brought new insights into the technology and the typology of the Lower and Middle Palaeolithic. Further new insights have been achieved by combining archaeological, geomorphological and lithostratigraphic studies. A chronological framework for the lithic industries found in these sites has been attempted, based on their stratigraphic position in the terrace deposits and by thermoluminescence (TL) dating (Mozzi et al., 2000). However, these TL dates from the Vale do Forno area were minimum age estimations. Furthermore, the validity/accuracy of these TL ages was unclear because of a lack of geochronological dating from other archaeological sites within reach IV (e.g. Raposo and Cardoso, 1998).

The main aim of this paper is to develop a new chronostratigraphy for the sedimentary succession of the Lower Tejo terrace T4 in the Vale do Forno area. A new and more robust chronologic framework will allows us to provide better dating of the Palaeolithic industries found here *in situ* and to estimate the duration of aggradation and down-cutting phases associated with this terrace. It will also allow correlation of these phases with extrinsic fluvial controls (climate, glacio-eustatic sea-level changes and tectonics). Finally, integration of the terrace sedimentology with an improved chronostratigraphic framework will allow a revised assessment of the palaeo-environmental conditions affecting this region of western Iberia during the Middle Pleistocene.

2. Geological setting

The study area mainly comprises siliciclastic sediments of the Lower Tejo Cenozoic Basin (LTCB), dominated by Miocene sediments on the western side and Pliocene sediments on the eastern side of the valley (Fig. 2). Eocene to Oligocene continental sediments outcrop along the western margin of the LTCB, forming a narrow fringe along a

thrust fault contact with Mesozoic limestones. The Neogene succession is composed of fluvial gravels, sands and silty clays, but also lacustrine/palustrine carbonates (Barbosa, 1995). Pleistocene sediments are represented by fluvial terraces, an aeolian cover unit (Carregueira Formation) and colluvium (e.g. Martins et al., 2009, 2010a, 2010b). Holocene sediments form an extensive alluvial plain, ca. 5 km wide at Alpiarça and up to 10 km wide in the downstream part of the study area. In reach IV, a deeply incised valley was excavated during the Marine Isotopic Stage (MIS) 2 sea-level fall, between 30,000 and 20,000 yrs ago; valley infilling occurred due to a combination of sea-level rise (20,000 to 7,000 yrs ago) and an increase in sediment supply, resulting from climate change and human impact (Van der Schriek et al., 2007; Vis et al., 2008, 2016; Vis, 2009).

3. Previous studies

Previous studies in reach IV by Breuil and Zbyszewsky (1942) and Zbyszewski (1943, 1946) identified only four fluvial terraces. These were represented in the 1/50,000 geologic maps using a stratigraphic framework based on the heights of terrace surfaces above river bed (a.s.l.): Q1 as +75–95 m; Q2 as +50–65 m; Q3 as +25–40 m and Q4 as +8–15 m. A glacio-eustatic model, based on the European Alpine glaciations, was used to explain the terrace formation as well as to provide a relative chronology. Q1 and Q2, the "upper terraces", were considered to relate to the Gunz–Mindel interglacial, or even to the pre-Gunz (Q1). Q3, the "middle terrace", was related to the late Mindel and the earliest Riss and Q4 (the "lower terrace") was ascribed to the Riss–Würm interglacial.

In more recent years the terrace stratigraphy in reach IV has been revised and now comprises six terrace levels (T1 is the uppermost and the T6 the lowermost; Corral, 1998a, 1998b; Martins, 1999; Rosina, 2002; Cunha et al., 2008; Martins et al., 2009, 2010a,

155 2010b). The additional terraces were recognised within the highest and lowest parts of the
156 landscape, the new highest terrace occurring above the original Q1 level and the new low-
157 est terrace occurring below the old Q4 level. Thus, the old Q1, Q2, Q3 and Q4 stratigraphy
158 has now been reclassified as the T2, T3, T4 and T5 terrace levels.

159 In the study area, two lithostratigraphic units were identified within the T4 terrace
160 (Mozzi et al., 2000): a "Lower Gravels unit" (LG) and an "Upper Sands unit" (US), which
161 are locally separated by a disconformity. The LG unit was linked to glacial conditions and a
162 sea-level lowstand, whereas the US unit was linked to an interglacial period of high sea
163 level.

164 No pre-bifacial (pre-Acheulian) assemblages have been found at the Vale do Forno ar-
165 chaeological sites or elsewhere in the Lower Tejo basin. The scarce lithic tools that were
166 found in the LG unit comprise crude bifacial forms attributed to an "Early Acheulian"
167 (Zbyzewski, 1946), but they are not sufficiently representative as to be ascribed to any spe-
168 cific Acheulian evolutionary phase. In the US unit, prolific industries represented by a
169 dozen sites have been registered since the 1940s, especially at Vale do Forno (VF) (Breuil
170 and Zbyszewki, 1942; Zbyzewski, 1946; Raposo et al., 1985; Mozzi et al., 2000; Raposo,
171 2002). One such example is the VF1 site, comprising a classic bifacial industry within a
172 thin gravel bed stratigraphically located in a lower sector of the US unit. The VF8 site is
173 located in a stratigraphically higher position and contains an industry dominated by small
174 to medium sized flake tools, but with some rare bifaces or biface-like tools. Finally, another
175 relevant industry has been found at site VF3, on a thin gravel bed located between a sandy
176 silt level at the top of the T4 terrace and an overlying aeolian-colluvial deposit. The VF3
177 industry, has traditionally been labelled as Micoquian and considered to represent the very
178 end of the Acheulian complex (Raposo et al., 1985).

For the Acheulian industries that have been recorded in the Upper Sands unit, Raposo (1995a) and Mozzi et al. (2000) proposed an age of ca. 150 to 70 ka, corresponding to the last interglacial/early phases of the last glacial (MIS 5 and the end of MIS 6). This is considerably younger than the age proposed by the previous studies, which linked the T4 terrace to the late Mindel and early Riss (ca. 400 to 300 ka). The younger chronology was based upon three arguments:

a) The occurrence of Micoquian industries at the VF3 site, these are extremely evolved, both from the technological and typological point of view;

b) The palaeoenvironmental interpretation of a spatially extensive floodplain succession with palaeosols and grey clays containing temperate floral fossils located below the upper Acheulian horizons. These fine-grained deposits were thought likely to indicate the Eemian transgressive episode;

c) The thermoluminescence (TL) dates obtained from the VF8 sequence. These provided minimum ages for three stratigraphic levels of the US: 117 ka (-26 ka + infinite), 119 ka (-32 ka + infinite) and >124 ka (Raposo, 1995a; Mozzi et al., 2000).

Correlations by Martins et al. (2010b) and Cunha et al. (2012), based mainly on geomorphologic criteria and new luminescence dating, indicated that the terrace containing the Lower Palaeolithic industries at Vale do Forno is equivalent to the T4 terrace of the upstream reach III (at Abrantes) and reach I (at Ródão) of the Lower Tejo. In these reaches, finite infrared stimulated luminescence (IRSL, from K-feldspar) and optically stimulated luminescence (OSL, from quartz) ages were obtained for the T4, T5 and T6 terrace deposits (Cunha et al., 2008, 2012; Martins et al., 2010a, 2010b): T4 – ca. 280 to 136 ka; T5 – ca. 136 to 75 ka; T6 - 62 to 32 ka. Thus the OSL ages for the T4 obtained in the upstream reaches can be used to constrain the age of the Vale do Forno industries. However, this time range should be regarded as a first estimate, since the ages of the T4 terrace were ob-

tained using the conventional low-temperature (50°C) IRSL signal method, for which the fading correction used (Lamothe et al., 2003) is not completely appropriate. This resulted in a significant underestimation for the oldest samples (Cunha et al., 2008; Martins, et al., 2009, 2010a, 2010b). Because of this age underestimation issue, Cunha et al. (2012) proposed that the T4 aggradation should probably range in age from 340 ka to 160 ka. In the present study, these limitations in luminescence dating are largely overcome by a new protocol that uses the elevated-temperature post-IRIR stimulation (Thomsen et al., 2008; Buylaert et al., 2009) for measuring samples that have the quartz-OSL signal in saturation. The $pIRIR_{290}$ dating method, using K-feldspar as the dosimeter, has negligible fading and can yield accurate results back to 600 ka (Buylaert et al., 2012).

4. Materials and methods

The information presented here is derived from geomorphological, stratigraphical, sedimentological and chronological data using a standard approach (e.g. Stokes et al., 2012): (1) a geomorphological study of the region, complemented by local detailed investigations and the generation of detailed maps using GIS, (2) field descriptions and stratigraphic correlation of the sedimentary units, (3) sedimentological characterization of the deposits and (4) luminescence dating.

Geomorphological mapping was undertaken in three stages: (1) field mapping onto topographical (1/25,000) and geological (1/50,000) base maps; (2) analysis of 1/25,000 black/white aerial photographs and of a digital elevation model (DEM) based upon a 1/25,000 topographic database; and (3) field ground truthing.

The T4 terrace deposits associated with the Vale do Forno archaeological sites and that of the equivalent alluvial sequence in the adjacent Vale de Atela sector were also studied in detail in order to improve our understanding of the local stratigraphy. Field work included stratigraphic logging and sedimentological characterization of the sedimentary deposits in order to obtain data on the depositional facies, including the sediment colour, texture, maximum particle size, clast lithology, fossil content, bedding and its overall depositional architecture. Soil features and horizons were described in the field, following international guidelines (Jahn et al., 2006).

Samples for OSL dating were collected from several Pleistocene sedimentary units that outcrop in the study area, namely fluvial sands of the T4 and T5 terraces and aeolian sands of the Carregueira Formation. A large number of different stratigraphic levels within the T4 terrace (from the base to the top) were sampled in order to improve the chronology of the terrace sequence and its associated lithic industries.

OSL dating is an absolute dating technique that measures the time elapsed since sedimentary grains of quartz or feldspar were last exposed to daylight (Duller, 2004). Exposure to daylight during sediment transport removes the latent luminescence signal from the quartz or feldspar crystals. After burial, the luminescence signal (trapped charge) starts to accumulate in the mineral grains due to ionising radiation arising from the decay of ^{238}U, ^{232}Th and ^{40}K present in the sediment itself and from cosmic ray bombardment. In the laboratory, the equivalent dose (D_e, assumed to be the dose absorbed since last light exposure, i.e. the burial dose, expressed in Gy) is determined by comparing the natural luminescence signal resulting from charge trapped during burial with that trapped during a laboratory irradiation. Dividing the D_e by the environmental dose rate (in Gy/ka) gives the luminescence age of the sediment. Environmental dose rates are calculated from the

radionuclide concentrations (U, Th, K) of the sediment. In this study, the radionuclide concentrations were measured by high-resolution gamma spectrometry (Murray et al., 1987). These concentrations were then converted to environmental dose rates using the conversion factors given by Olley et al. (1996). For the calculation of the dose rate of sand-sized K-feldspar grains an internal K content of 12.5±0.5% was assumed (Huntley and Baril, 1997). Sampling tubes were hammered into previously cleaned outcrops. Immediately adjacent to each tube, a sub-sample of sediment was collected for determination of field water content, saturation water content and dose rate.

Sample preparation for luminescence analyses was done in darkroom conditions. Samples were wet-sieved to separate the 180–250 μm grain size fraction followed by HCl (10%) and H_2O_2 (10%) treatments to remove carbonates and organic matter, respectively. The K-feldspar-rich fraction was floated off using a heavy liquid solution of sodium polytungstate (ρ = 2.58 g/cm^3). The quartz fraction was obtained by etching another portion with concentrated HF (40%). The K-feldspar fraction was treated with 10% HF for 40 min to remove the outer alpha-irradiated layer and to clean the grains. After etching, both the quartz and K-feldspar fractions were treated with HCl (10%) to dissolve any remaining fluorides. Quartz purity was confirmed by the absence of a significant infrared-stimulated luminescence (IRSL) signal.

Equivalent doses were measured on automated Risø TL/OSL DA- 20 readers, each containing a beta source calibrated for irradiation on stainless steel discs and cups. Quartz measurements were made on large (8 mm) aliquots containing several thousands of grains mounted on stainless steel discs. Small (2 mm) aliquots of K-feldspar were mounted on stainless steel cups.

Quartz dose estimates were made using a standard SAR protocol using blue light stimulation at 125°C for 40s with a 240ºC preheat for 10 s, a 200ºC cut heat and an elevated

temperature (280°C) blue-light stimulated clean-out step (Murray and Wintle, 2000, 2003). The OSL signal was detected through a U-340 filter. All samples have a strong fast component. The net OSL signal was calculated from the initial 0.0-0.8 s of stimulation and an early background between 0.8-1.6 s.

The K-feldspar D_e estimates were measured with a post-IR IRSL SAR protocol using a blue filter combination (Thomsen et al., 2008; Buylaert *et al.*, 2012). The preheat was 320°C for 60 s and the cut-heat 310°C for 60 s. After preheating the aliquots were IR bleached at 50°C for 200 s (IR_{50} signal) and subsequently stimulated again with IR at 290°C for 200 s ($pIRIR_{290}$ signal). It has been shown by Buylaert *et al.* (2012) that the post-IR IRSL signal measured at 290°C can give accurate results without the need to correct for signal instability. For all IR_{50} and $pIRIR_{290}$ calculations, the initial 2 s of the luminescence decay curve less a background derived from the last 50 s was used.

5. Results

5.1 Terrace staircase

In the study area, the culminant sedimentary surface (CSS) is the surface of the Serra de Almeirim Conglomerates (Barbosa, 1995). This uppermost sedimentary unit of the LTCB, and the upstream equivalent in Portugal, represented by the Falagueira Formation (Cunha, 1992, 1996), has been considered of latest Zanclean to Gelasian age (3.65 to 1.8 Ma; Cunha et al., 2012, 2016; Pais et al., 2012; Diniz et al., 2016). Previous studies (e.g. Cunha, 1992, 1996; Cunha et al., 1993, 2005, 2016) indicated that by ca. 3.65 Ma (end of the Zanclean) the westward draining Atlantic fluvial drainage (in the Lower Tejo basin), during a period of high sea-level (up to +40 m), also received drainage from the previous endorheic Madrid Cenozoic basin (e.g. Pérez-González, 1994). Our interpretation considers a spill-over drainage model (e.g. Douglass and Schmeeckle, 2007) as responsible

for the change of the Douro and Madrid Cenozoic basins from endorheic to exorheic: when the hot climate of the Pliocene became very humid, the large water level increase in each endorheic basin (forming a huge lake) induced an overspill towards the west, to the lower Atlantic Ocean.

Ongoing studies indicate that in the Lower Tejo Basin the incision stage began by 1.8 Ma (Cunha et al., 2012, 2016), controlled both by climate (global cooling; see, e.g., Bridgland and Westaway, 2014), eustasy (sea-level lowering) and tectonics (ongoing crustal uplift since 9.5 Ma due to Iberia-Africa convergence) (e.g. Cunha, 1992; Cunha et al., 1993, 2016; De Vicente et al., 2011). During the subsequent fluvial incision, the Lower Tejo and its tributaries developed a staircase of six terraces into the fill of the LTCB (Fig. 3).

In the study area (Vale de Cavalos – Muge; Fig. 3), only five terraces are represented because the T6 terrace is buried by Holocene alluvium. The staircase can be characterized as follows (Table 1):

- The remnant surface of Serra de Almeirim conglomerates (CSS) is at ca. 133 m a.s.l. (+123 m, above river bed, a.r.b.) at Alpiarça; the unit has a thickness of ca. 35-40 m and consists of fluvial gravels interbedded with coarse sands;

- The T1 terrace is at ca. 115 m a.s.l. (+107 m) around Vale de Cavalos (upstream) and at ca. 90 m a.s.l. (+86 m) around Muge (downstream) (Fig. 3). T1 has a maximum thickness of ca. 5 m, and is made up of reddish gravels overlying the Miocene substratum.

- T2 is represented by the terrace treads at 82 to 72 m a.s.l. (+74 to 68 m). The T2 is a 6 -7 m thick fill terrace, mainly composed of brown massive clast-supported gravels.

- T3 terrace is at 60 to 50 m a.s.l. (+52 to 46 m). It is well preserved on the north side of the Muge stream where it is ca. 10 m thick.

- T4 terrace is at 38 to 20 m a.s.l. (+30 to 16 m). It forms a 5 km long ramp, rising from 20 to 40 m a.s.l. north of the Muge stream. Boreholes for water extraction and the available

outcrops indicate that the T4 has a maximum thickness of ca. 30 m at Alpiarça (Mozzi et al., 2000) and ca. 23 m near Muge.

- T5 terrace forms a narrow strip at 13 to 10 m a.s.l. (+3 to 6 m), between Vale de Cavalos and Muge. In the study area, the base of T5 is below the top of the modern alluvial plain but downstream of Muge, the whole T5 thickness is buried by the Holocene valley fill; boreholes indicate a thickness of 9-10 m.

- Boreholes indicate that the T6 terrace top is at -4 m a.s.l. and is ca. 18 m-thick.

- A late Pleistocene aeolian sand unit (Carregueira Formation), usually <3 m-thick, locally covers the T5 and T4 terraces.

- Boreholes revealed a ca. 30 m-thick Holocene succession (Vis, 2009).

The lithostratigraphy of the T4 terrace was described by Mozzi et al. (2000) (Figs. 4, 5 and 6). In the present study additional data were collected, with three stratigraphic logs being obtained from Vale do Forno and Vale de Atela (Fig. 7). Figure 8 shows the sand-pit (27 m high) used to produce the Vale de Atela-E log (Fig. 7).

Outcrops of the LG unit show a minimum thickness of 10 m, but the overall maximum thickness appears to be 13-15 m based upon water-well stratigraphy. The unit is made of subrounded to subangular gravels of quartzite (predominant) and quartz, with a coarse sandy matrix. The sediments usually occur as clast-supported imbricated gravels that display a crude horizontal bedding (lithofacies Gh), interpreted as longitudinal fluvial bars deposits. Locally, some small channel geometries can be seen and lenses of other facies can be intercalated with the dominant Gh. These include the lithofacies Gp, characterized by gravel with planar cross-beds, interpreted as transverse fluvial bars, and lithofacies Sm, comprising massive medium sand, interpreted as deposited by turbulent fluvial currents. The LG unit deposits are interpreted as corresponding to a gravelly braided fluvial system,

355 transporting a coarse bed load (average maximum pebble size of 14 cm, but with rare
356 boulders reaching 30 cm in diameter).
357 The US unit has a maximum thickness of 20 m. The basal 2-4 m of the unit (Fig. 7)
358 comprises either (1) massive and pebbly coarse sands (lithofacies Sc) or (2) trough cross-
359 beds (lithofacies St). These represent bed-load transport of sand, mainly as sinuous-crested
360 fluvial dune bedforms. The middle part of the US unit (ca. 6-10 m) consists of very thick
361 (up to 5.5 m) massive grey clayey silts (lithofacies Fm) that locally contain small
362 fragments of coal. The silts are intercalated with thin beds (<1 m) of massive medium to
363 fine yellowish sands (lithofacies Sm). Collectively, this alternation of silts and fine sands is
364 interpreted as overbank deposits comprising crevasse splays (Sm) and backswamp deposits
365 (Fm). Leaves of *Salix* and rhizomes of *Nymphea* (Zbyszewski, 1946) and a pollen content
366 limited to *Ericacea* and *Pinus* (Montenegro de Andrade, 1944) have been reported in the
367 backswamp deposits. The backswamp deposits document a marked decrease in fluvial
368 energy and the formation of an extensive flood-plain adjacent to channel deposits to the
369 west (Fig. 5). The upper part of the US unit (ca. 8-9 m) is dominated by tabular beds (Fig.
370 8) of lithofacies Sc and Sm, with rare thin intercalations of facies Fm. Thus, the upper part
371 of the US unit indicates that the environment changed to a system dominated by sand flats
372 and large bars.
373
374 The <2 μm fraction of the US overbank deposits have as clay minerals essentially
375 montmorillonite/vermiculite, associated with kaolinite and illite (Mozzi et al., 2000); a
376 significant part of these clay minerals could be sourced from erosion of the local Neogene
377 sedimentary units. Zbyszewski (1946) interpreted the US macrofloral assemblages to
378 indicate a mild-temperate climate similar to that of the present day.

Palaeosols within the US unit provide some information regarding drainage and climate conditions. A trench (Fig. 9) excavated at location AL1 (see Fig. 4), records three separate palaeosols in lithofacies Fm, positioned in the middle part of the US unit between 27 and 21 m a.s.l.. Each palaeosol can be traced over a wide area of some 4 km^2, being observed in numerous sections. The main palaeosol characteristics are reported in Table 2. All palaeosols show abundant mottles and coatings of Fe-Mn oxides along cracks and on the faces of soil aggregates, as well as slickensides and pressure faces in the more clayey horizons. These features are indicative of poorly drained soils within a fine-grained floodplain (Aslan and Autin, 1998). Slickensides and pressure faces suggest the occurrence of significant variations in soil water content (Dinka et al., 2013), implying strong seasonal variability with summer drought. Palaeosols displaying seasonal wet-dry cycles cover an area of several square kilometers, which suggests that they are not localized occurrences associated with periodic channel levee breaching. Instead, each palaeosol seems to be indicative of wider floodplain stability and, thus, corresponds to a potential hiatus in the sedimentary sequence. The degree of evolution of the palaeosol profile may provide some clue as to the time scale involved in its formation (Huggett, 1998; Zielhofer et al. 2009). For example, the observed palaeosol characteristics can commonly form in relatively short time spans, possibly in the order of 10^3-10^4 years (Yaalon, 1983). Nevertheless, it must be pointed out that the hydromorphic setting in which soil formation occurred is not adequate for producing unequivocal soil chronosequences, as the soil hydrology is expected to be a major controlling factor which may severely limit the evolution of the soil profile. As time may not be a predominant factor, the above time intervals should be regarded only as minimal age constraints.

5.2 Lithic industries

The supposedly "Early Acheulian" industries were found in the LG unit by Zbyszewsky (1946). Part of this unit is presently submerged by a local dam and for the last two decades it has not been possible to find additional artefacts *in situ*.

In contrast, archaeological sites are numerous in several stratigraphic levels within the US unit. Acheulian industries, containing "large cutting tools", such as bifaces, cleavers and sidescrapers are present. Clear Middle Palaeolithic industries, the so-called "flake industries" or Mousterian, based on specific core reduction sequences (mainly discoid or Levallois), with no relevant occurrence of large cutting tools, are almost absent. In contrast, bifaces and cleavers do occur throughout the alluvial sequence, evolving technologically and typologically. Here, we summarize the three main archaeological sites excavated from the US unit in the Vale do Forno area, described in stratigraphic sequence (VF1, VF8 and VF3). The large number of artefacts discovered allows for a cultural diagnosis of the industries.

The VF1 site (Vale do Forno; Figs. 4 and 6) was found in the lowermost in the stratigraphy, within the basal channel sandy deposits of the US unit. Typologically, the lithic industry is represented by poorly evolved Acheulian tool types (Fig. 10). It contains a high percentage of flaked pebbles, unifacial choppers and hand axes, all of a quite rough manufacture; flakes show few implements.

At the VF8 site (Vale do Forno; Figs. 4, 5, 6, 7, 11 and 12) artefacts were recovered from the upper part of the US unit from a fine sand level (facies Sm) and an immediately overlying clayish silty bed (Fm). Approximately three thousand artefacts have been recovered from a thin archaeological horizon (ca. 10 cm-thick) interbedded in clays. A high concentration of flaked lithic materials (~140 artefacts per m^2 from an excavated area of 20

m^2) and the presence of the entire reduction sequences, from manuports and tested cobles, cores, initial flakes and large tools up to small retouched tools and abandoned debris, documents both the integrity of the site and the fact that local flaking activities were taking place in a flood-plain environment. Final retouched tools represent 15% of the total industry including waste products (or 24 % without them). This observation is even more significant giving that finished tools represent more than 30% of the total weight of the lithic products, something that is directly related to the presence of the characteristic Acheulian large cutting tools. These large Acheulian tools are almost residual in numeric terms: 5 % of bifaces and cleavers ("hachereaux") and 9 % of choppers and chopping-tools. Most of the retouched artefacts are retouched tools on flake (84 % in numeric terms; 42 % concerning weight), dominated by notches and denticulates, sidescrapers, dorsal knives, borers and "becs" (a Palaeolithic flake boring tool retouched on one edge to form a point). Discoid centripetal reduction sequences are rare and the *Levallois* method is absent.

The VF3 site (Milharós, Fig. 4) provided an assemblage of artefacts found on a thin layer located between a fluvial sandy silt level at the T4 terrace top and a colluvial deposit associated with aeolian sands (Raposo, 1996). After the archaeological excavation, a camping site (Fig. 6) was constructed on the VF3 site and later sampling for luminescence dating was not possible. However, the VF3 industry postdates the T4 terrace and predates the deposition of the Carregueira Formation (the aeolian unit covering the terrace). This stratigraphic position is important for understanding the likelihood of a much younger age for this typologically much evolved Acheulian industry, the so-called Micoquian. The VF3 lithic industry is mainly of quartzite composition with the most important typological groups being: bifaces (8 %) cleavers (4 %), side-scrapers (9 %), pebble tools (15 %), flake tools (9 %), cores (13 %) and flakes (42 %) (Figs. 13 and 14).

455 This degree of evolution and the highly standardized character of the bifaces that are
456 made from quartzite, indicate that the raw material did not constitute an impediment to
457 producing evolved tools. The level of sophistication is similar to that of bifaces
458 manufactured from flint, a raw material that is much more favorable for long knapping and
459 retouching sequences than quartzite. Typologically (according to the Jacques Tixier
460 system) cleavers from the VF3 appear to be quite "primitive". However, this primitiveness
461 is probably more apparent than real, and is probably related to the nature of the typological
462 system in use – this is mainly technologically oriented, rather than morphologically
463 oriented as it is more common in all traditional typological systems. In fact, due to the
464 absence of the *Levallois* method and its corresponding flaked products, all cleavers are
465 made on large entirely cortical or semi-cortical flakes, obtained from large cobles. These
466 flakes have been referred to as "Acheulian flakes" since the 1940s (Zbyszewski, 1943).
467 These flakes comprise a much more standardised support, either in terms of thickness
468 indexes as in term of elongation indexes. The flaking platform is almost always cortical
469 (rarely planar) and is often laterally situated, tending sometimes to the lower, proximal
470 sector of the flake. From a strictly morphological point of view, the cleavers made on these
471 flakes are as evolved as the bifaces (Raposo, 1996). They show high degrees of symmetry,
472 corresponding to what can be considered the geometrical "mental template" of the
473 prehistoric artisan. So, the differences between "evolved" bifaces and apparently
474 "primitive" cleavers seems to derive from the intention of the Acheulian artisan to use a
475 more complex reduction sequence to obtain the bifaces (successive retouch and edge
476 refining) and to adopt a very limited knapping sequence to produce cleavers. The
477 difference between the refinement procedures of the bifaces and cleavers seems to be more
478 related to the system of classification used: a system oriented to the morphological

evaluation, in the case of the bifaces, and a system of classification oriented to the evaluation of the technological procedures, in case of cleavers.

Recently published evidence from Britain recognizes assemblages with these same two distinctive handaxe types (cleavers and 'lanceolate' forms) in combined assemblages dating from around Marine Isotope Stage (MIS) 9, with the chronology based on the position of such assemblages within the well-dated sequence of the Thames and its tributaries (Bridgland and White, 2014, 2015). This new evidence arises from a reappraisal of high-integrity assemblages of handaxes recognized by Roe (1968) (also see Chauhan et al., this volume).

However, the VF3 bifaces are also similar to those found in the Manzanares Valley Complex Terrace of Butarque (near Madrid, ~400 km away), which Middle Palaeolithic stone tools have been dated to between the final Middle Pleistocene (MIS 6, 190-130 ka) and the early Late Pleistocene (MIS 5, 130-71 ka) (Panera et al., 2014), but also in several other areas of the Iberian Peninsula, where more evolved tools, such as lanceolate bifaces and Micoquian forms, surpass the more "primitive" ovate and amygdaloid forms.

Based on the above discussion, we consider that the VF3 industry is likely to represent an occupation on the surface of the US shortly after its deposition.

5.3 Luminescence dating

Quartz-OSL could only be applied to one palaeosample (132201) and to the two modern river bed samples (102232, 102263); for all the other samples the quartz natural OSL signals are too close to saturation to be useful for dating. For these older samples, signals from K-rich feldspars were used instead because of the higher saturation dose of the feldspar dose response curve (inset Fig. 15a; D_0 of ~500 Gy, compared to typically ~80 Gy for fast OSL component in quartz (Wintle and Murray, 2006). The $pIRIR_{290}$ signal from

feldspar was chosen because of its stability (Buylaert et al., 2012). We have also undertaken several direct tests of the stability of the $pIRIR_{290}$ signal, the suitability of the applied measurement protocol and the completeness of bleaching of this signal at deposition.

Buylaert et al. (2012) have suggested the use of first IR stimulation plateaus to examine the stability of the $pIRIR_{290}$ signal. We have measured such a plateau for sample 102226 collected in the T1 terrace, estimated to have an age of ca. 1.1-0.9 Ma by ESR and OSL dating of the terrace staircase (Cunha et al., 2012, 2016; Rosina et al., 2014; Martins et al., 2010a, 2010b). This sample is old enough that its natural $pIRIR_{290}$ signal is expected to lie at or close to the saturation in the dose response curve (samples of so-called non-finite luminescence age). The ratio of natural $pIRIR_{290}$ signal to the saturation level of the dose response curve varies between 0.93 and 0.95 for first IR stimulations varying between 50°C and 230°C. This demonstrates that the $pIRIR_{290}$ signal is sufficiently stable for dating (effects of fading in nature <10%) and we have adopted 50°C as a suitable prior IR stimulation temperature.

The reliability of the SAR $pIRIR_{290}$ dose measurement protocol was further tested using a dose recovery test based on two modern river bed samples (102232 and 102263). Laboratory beta doses ranging from ~15 to ~800 Gy were added to natural aliquots of these two samples and measured in the usual manner. The measured doses (after subtraction of the small natural dose) are plotted as a function of the given laboratory doses in Fig. 15b. It can be seen that large laboratory doses, given prior to heat treatment, can be accurately recovered with this protocol.

It is obviously important to be confident that the $pIRIR_{290}$ signal was well-bleached at deposition. For the single aeolian sample (132201) the agreement with the quartz age control confirms adequate bleaching prior to deposition. For the fluvial samples we have

two lines of argument. First of all we have taken two sand samples currently in transport from the modern channel (102232 and 102263) and these both give $pIRIR_{290}$ D_e values ≤ 20 Gy, small or negligible compared with the other fluvial doses in this study (between 180 Gy and saturation). Secondly, Murray et al. (2012) and Buylaert et al. (2012, 2013) have shown by exposing natural samples to artificial sunlight for different lengths of time that the $pIRIR_{290}$ signal bleaches much more slowly than the IR_{50} signal. This differential bleaching rate can be used to identify samples for which the $pIRIR_{290}$ signal is likely to be well-bleached (Murray et al., 2012; Buylaert et al., 2013). Fig 15c shows the IR_{50} D_e values as a function of the $pIRIR_{290}$ D_e values. The data are consistent with a smooth curve passing through the origin. The absence of obvious outliers suggests that all $pIRIR_{290}$ signals were probably well-bleached at deposition in comparison with their subsequent burial doses. It could be argued that the two samples lying below the line on the $pIRIR_{290}$ axis might suggest incomplete bleaching of the $pIRIR_{290}$ signal. But we are fortunate that the sample (102233; 81±4 ka) lying immediately above the layer with independent U-series age control (81.9 +4.0/-3.8 ka; Raposo, 1995a) lies in this group, clearly confirming that this sample was adequately bleached. The sample immediately below (102263; 75±14 ka) is also consistent with the age control and with a $pIRIR_{290}$ D_e of 200±35 Gy lies on the smooth line (Fig. 15c).

Six out of the nineteen samples reported in Tables 3 and 4 have D_e values lying above $2xD_0$ (corresponding to 86% of luminescence saturation). Especially in view of the possibility of small systematic errors in the measurement of the luminescence signal (Fig. 15a), we feel it prudent to adopt the strategy suggested by Wintle and Murray (2006) of only presenting minimum doses for these samples (equivalent to $2xD_0$) and the derived minimum ages. We also note that our measurement protocol has only been tested against independent age control up to ~$2xD_0$ (Buylaert et al., 2012).

555 To constrain the artefacts stratigraphically, most of the samples were collected in T4, at the
556 Vale do Forno and Vale de Atela sections (Fig. 4). Others samples were collected in
557 outcrops of T5 (Figs 3 and 16), one sample in the aeolian sands of the Carregueira
558 Formation and two samples from the river bed (modern). The luminescence dating results
559 are all summarised in Tables 3 and 4.
560 As stated above, dating by the $pIRIR_{290}$ protocol was tested using two samples from the
561 topmost deposits of the T5 terrace of a Tejo tributary, at Santo Antão do Tojal (near Vila
562 Franca de Xira; Fig. 2) from which a large elephant bone was collected and dated by using
563 the U/Th series (Raposo, 1995a). The $pIRIR_{290}$ ages of the samples Atojal-1 and Atojal-2
564 (Table 4), taken from the same stratigraphic levels, corroborate the independent age
565 obtained by the U/Th series (81.9 +4.0/-3.8 ka).
566 Sample 132203 (Atela 3) was collected in the LG unit, from a gravel pit situated in the
567 right-bank (northern side) of the Vale de Atela (V.Atela-W) (Figs. 4, 5 and 7).
568 Stratigraphically, it is the lowest sample of the terrace T4 (LG – middle part), collected in
569 the Alpiarça area. Because the natural $pIRIR_{290}$ signal is in saturation only a minimum age
570 of >200 ka is given (Table 4).
571 The samples collected at the base of the US unit (AM-22 and VCaval-1) all gave minimum
572 ages, respectively of >270 ka and >200 ka. Sample 052216 (AM-15) (>270 ka) was taken
573 below the levels containing the Late Acheulian artefacts of the VF8 site and the other
574 samples from sites located far away (Figs. 3, 4 and 17), but in an equivalent stratigraphic
575 level of the sample AM 15.
576 From the middle part of the US unit a minimum age (AM-21; >300 ka) and a finite age
577 (VForno 8-2; 201±16 ka), were obtained. The VForno 8-2 sample is located 4 m above the
578 stratigraphic level containing the VF8 artefacts (Figs. 4, 6, 7) and therefore the artefacts of
579 the VF8 site are older than 200 ka and, probably somewhat older than 300 ka.

Sample Atela 2 (132202) was collected at ca. 2.5 m below the local eroded surface of the T4 terrace and provided a minimum age (>200 ka). The samples VForno-1 (132244) and VForno-2 (132245) were collected at the T4 topmost deposits (Figs. 4 and 7) and gave ages of 158 ± 9 and 154 ± 10 ka, that are according to stratigraphy.

Throughout the T4 sequence, the finite luminescence ages are always in stratigraphic order. Due to the high dose rates, the LG unit and the base of the US unit were found outside the upper range of the $pIRIR_{290}$ method. Sediments of the middle and upper part of the US unit provided finite ages (not minimum) only occasionally. The topmost deposits of the T4 terrace are on the threshold of the dating method and have an age of ca. 155 ka.

In summary, the new $pIRIR_{290}$ ages for the T4 deposits in the study area indicate that:

1) The LG unit, containing the artefacts reported by Zbyszewsky (1946), has an age much older than 300 ka;

2) The lower and middle part of the US unit, containing the VF1 and VF8 Acheulian industries, has a probable age of ca. 330 to 200 ka;

3) The upper part of the US unit has an age of 200 to 155 ka.

Samples Muge-1 (PC5239), Muge-2 (PC5240) and PSabug-2 (102231), collected from the T5 top deposits (Fig. 16), yielded ages of ca. 95 to 75 ka.

The sample Azinh-3 (39 ± 2 ka), taken from the topmost deposits of the terrace mapped near the village of Azinhaga (Fig. 3), confirms the geomorphological correlation of this terrace with the T6 level. From other luminescence dating studies, the T6 terrace has been dated as ca. 65 ka (base deposits) to ca. 32 ka (top deposits) and correlated with MIS 3 (Martins et al., 2010a, 2010b; Cunha et al., 2008, 2012).

Finally, the aeolian sands of the Carregueira Formation, that covers the T5 and T4 terraces in the study area, was dated at Almeirim (sample Almer-1; 132201) as 19.1±1.1 ka (Quartz-OSL).

6. Discussion

In an environment of continuous uplift, the formation of fluvial terraces has been correlated with climate changes (e.g. Gibbard and Lewin, 2002; Bridgland and Westaway, 2008; Bull, 2009) but lower reaches could be dominated by sea-level changes (e.g. Merritts et al., 1994; Blum and Törnqvist, 2000; Lewis et al., 2004). The data obtained in the study area indicate that the terrace aggradation episodes can be correlated with the Marine Isotope Stages (MIS; e.g. Wright, 2000; Lisiecki and Raymo, 2005). Being much older than 300 ka, the LG unit most likely corresponds to the earlier part of the MIS 9 (337 to 325 ka), immediately postdating incision promoted by the very low sea level (reaching ca. -140 m) during MIS 10 (362 to 337 ka) (Fig. 17). This suggests that the aggradation of the coarse-grained T4 terrace base has probably occurred during a period of low sea level and relatively cold climatic conditions (e.g. Gibbard and Lewin, 2002), probably marked by sparse vegetation cover on slopes (Roucoux et al., 2006). This climate relationship for valley floor aggradation is typical of many large European river systems (e.g. Bridgland and Westaway, 2008). During the post-MIS 10 period, sea level was rising fast (Murray-Wallace and Woodroffe, 2014). The sedimentary architecture of the amalgamated channel deposits of the LG unit seems compatible with the ca. 335 to 325 ka age estimate, as it suggests a coarse bedload river with high sediment supply.

The lower and middle parts of the US unit, comprising alternations of clayey silts, sands and palaeosols on clays to the east (flood-plain deposits) and dominant sand deposits to the west (channel belt), have a probable age of ca. 325 to 200 ka. This suggests formation during a period spanning MIS 9 through to MIS 7 (Fig. 17). This time period was characterised by: (i) high to medium sea levels (Murray-Wallace and Woodroffe, 2014); (ii) warm to

mild climatic conditions (the interstadials of the MIS 7 were similar to the present Mediterranean climate) intercalated with a cold period during the late part of the MIS 8 (Roucoux et al., 2006; White et al., *in press*).

The sandy upper part of the US unit, with a probable age of 200 to 155 ka, seems to relate to the early part of MIS6 (Fig. 17). In this period, climate deterioration and a relative depletion of vegetation cover would have allowed enhanced sediment production in the catchment, while progressive sea-level lowering increased the longitudinal valley slope. This would have resulted in down-valley progradation of coarse grained fluvial deposits along the Tejo valley. Within the study area this is recorded by the covering of the fine-grained floodplain deposits by the sandy deposits of the upper part of the US unit.

The T5 terrace, located immediately below the T4, represents the MIS 5 in reach IV, and is correlated with the same terrace level in the upstream reaches of the Lower Tejo (ca. 135 to 75 ka). This time period was characterised by high to medium sea-levels (Fig. 17) and warm to mild climatic conditions (Salgueiro et al., 2010).

The Carregueira Formation is an aeolian sand unit represented in several reaches of the Lower Tejo valley and can be related to the cold and dry climatic conditions that occurred between ca. 32 and 12 ka, during the Last Glacial period (MIS 2; Roucoux et al., 2005; Martins et al., 2010b; Cunha et al., 2012) (Fig. 17).

Additional palaeoenvironmental interpretations concerning the genesis of T4 can be made using the palaeosols that occur interbedded in the clays at the top of the middle part of US unit (Figs. 9 and 17). Their position, just above the VF8 archaeological level and below the level of the VForno8-2 sample, suggests a period spanning ca. 300 to 200 ka. The mottles and concretions within these soils, together with the presence of well-developed pressure faces and slickensides in the more clay rich horizons, suggest that the soils were subject to

alternating wetting-drying cycles (Pal et al., 2009; Vepraskas and Lindbo, 2012). This hydromorphic interpretation is compatible with the position of soils within a fine-grained floodplain setting where the water table is close to the surface. Nevertheless, the variation of soil humidity suggests a strong seasonal variability in the floodplain, with waterlogged conditions presumably related to winter rain and flooding, and drying-up during the summer. Such a hydrological regime, typical of the Mediterranean climate, is consistent with palynological data from offshore Portugal (Roucoux et al., 2006), where forest expansions with a significant contribution from the Mediterranean floral elements were recorded during the three warm sub-stages MIS 7a, 7c, and 7e, that occurred between 243 and 185 ka (Fig. 17).

Each palaeosol represents a hiatus in the alluvial sequence and indicates a period of floodplain stability. Forest expansion in MIS7 warm sub-stages would be favourable to lower sedimentation rates in the alluvial plain, with deposition dominated by fines, and palaeosol development. In turn, the cold and dry sub-stages with pronounced contraction of tree populations would be favourable to slope erosion and increased sedimentation rates on the alluvial plain, with deposition dominated by sands. The minimum time for formation of each palaeosol is thought to be of the order of 10^3-10^4 years (Yaalon, 1983), consistent with the duration of sub-stages. A future detailed sampling in stratigraphy, for absolute dating, could address this topic.

Previous studies in the Alpiarça area linked the T4 US unit to the Late Riss to Early Würm period of the Alpine chronology (i.e. ca. 150 to 70 ka). This chronology was mainly based on the technical and typological refinement of the VF3 site industry and on the TL minimum ages then obtained (Raposo, 1995; Mozzi et al., 2000). Additionally, chronological constraints were also based on local and regional geomorphological

680 considerations. However, the new luminescence ages presented within this study suggests
681 the basal and middle parts of the US unit, containing the Middle and Late Acheulian VF1
682 and VF8 sites, are likely to be much older, ca. 310 ka.
683 The lithic industry of the VF3 site should not be considered as belonging to the alluvial
684 sequence of the T4 terrace, as already discussed by Raposo (1996). The VF3 artefacts were
685 worked on the T4 surface and were later covered by a colluvium and aeolian sands. If this
686 colluvium can be ascribed to the base of the Carregueira Formation, with an age of 32 to
687 12 ka and containing *in situ* Late Palaeolithic artefacts (Cunha et al., 2012), the VF3
688 industry should be younger than ca. 155 ka but much older than 32 ka. Based on the
689 typology of the handaxes, the age of this industry could not be much younger than 155 ka.
690 In the Middle and Upper Tejo/Tajo (in Spain) a maximum of 16 "true" fluvial terraces (not
691 considering fan-head trench terraces) have been identified and dated by combining
692 absolute ages and paleomagnetic data (Silva et al., 2016): (i) the first Palaeolithic materials
693 are represented by isolated large flint flakes of apparent early Achaeulian fracture, and
694 these are associated with the +100-107 m to +80-85 m terraces (probably with ages ca. 1.4-
695 1.2 Ma); (ii) Achaeulian sites were found in terraces ranging from +70-78 m (probably ca.
696 1.1-1.0 Ma) to +18-22 m (ca. 135 to 74 ka), the later terrace has upper stratigraphic levels
697 containing Middle Palaeolithic industry with Mousterian knapping technology; (iii)
698 Mousterian sites were found in terraces between +15-13 m to +8-10 m (ca. 60 to 28 ka)
699 (e.g. Santonja and Pérez-González, 2010; Pérez-González et al., 2013; Panera et al., 2014;
700 López-Recio et al., 2015; Roquero et al., 2015a, 2015b; Rubio-Jara et al., 2016). The most
701 complete list of artefacts associated with a warm faunal assemblage was found in the
702 Achaeulian sites of Pinedo and Cien Fanegas (Tagus valley, near Toledo) in the +25-30 m
703 terrace, with top deposits dated as 226±37 ka (by Amino-Acid Racemization) and the base

deposits dated as >280 ka and 292±17 ka (pIR-IRSL) (López-Recio et al., 2013, 2015). So, this terrace of the Middle Tejo correlates well with the Lower Tejo T4 terrace.

However, there are not enough reliable and precise absolute ages to support a detailed correlation between the staircases of the Middle and Upper Tejo/Tajo (in Spain, up to 16 fluvial terrace levels) and the Lower Tejo (in Portugal, only 6 terrace levels). We should also note that the sedimentary controls for the formation of the Lower Tejo staircases are different (mainly glacio-eustasy and differential uplift) and that the Lower Tejo is separated from the Middle and Upper Tejo by a large permanent knick zone of hard basement (Cunha et al., 2016; Silva et al., 2016). The ages already obtained from the terraces of the lower reach of the Portuguese Mondego River (Ramos et al., 2012) seem to correlate well with the Lower Tejo River terraces; both of the river reaches seem to have glacio-eustatic control on their development.

7. Conclusions

Geomorphological analysis of the Lower Tejo reach IV confirms the existence of six sedimentary terrace levels, discontinuously represented along the entire of the Lower Tejo valley. In the upstream reaches I and III, six terrace levels have already been recognized by previous workers. Longitudinal correlation between these terraces indicates that a graded profile ca. 200 km long was achieved during terrace formation periods and a strong control by marine base level was a key determinant for terrace formation.

In the study area, the sedimentary units of the T4 terrace seem to record the fluvial response to sea-level changes and climatically-driven fluctuations in sediment supply.

The thick, coarse and dominantly massive gravels of the LG unit indicate deposition by a coarse bed-load braided river, with strong sediment supply, high gradient and fluvial com-

729 petence, during conditions of rapidly rising sea level. Luminescence dating only provided
730 minimum ages but it is probable that the LG unit corresponds to the earlier part of the MIS
731 9 (337 to 325 ka), immediately postdating the incision promoted by the very low sea level
732 (reaching ca. -140 m) during MIS 10 (362 to 337 ka), a period of relatively cold climate
733 conditions with weak vegetation cover on slopes and low sea level.
734 The lower and middle parts of the US unit, comprising an alternation of clayish silts with
735 palaeosols and minor sands to the east (flood-plain deposits) and sand deposits to the west
736 (channel belt), have a probable age of ca. 325 to 200 ka. This suggests formation during
737 MIS 9 to MIS 7, under conditions of warm to cold conditions and a high to medium sea
738 level.
739 The upper part of the US unit, dominated by sand facies and with an age of ca. 200 to 155
740 ka, correlates with the early part of the MIS 6. During this period, fluvial aggradation and
741 progradation resulted from climate deterioration and relative depletion of vegetation that
742 promoted enhanced sediment production in the catchment, coupled with initiation of sea-
743 level lowering that increased the longitudinal slope.
744
745 The oldest artefacts previously found in the LG unit, display crude bifacial forms that can
746 be attributed to the Acheulian, with a probable age of ca. 335 to 325 ka.
747 The VF1 and VF8 Acheulian industries, situated in the T4 US unit, probably date 325 to
748 300 ka. Notably, these Lower Palaeolithic artisans were able to produce tools with different
749 levels of sophistication, simply by applying different strategies. More elaborated reduction
750 sequences were used in case of bifaces, and simpler reduction sequences to obtain cleavers.
751 The VF3 artefacts were abandoned on the T4 surface and later covered by a colluvium and
752 aeolian sands. This industry is younger than ca. 155 ka but much older than 32 ka; we

consider that the VF3 industry should be interpreted as representing an occupation on the T4 surface shortly after the end of deposition.

The differences observed in the lithic assemblages documented at each of these sites can be attributed to a certain degree to particular economic functionalities. But, simultaneously, taking into account the stratigraphic position of these sites and the global technological and typological characteristics of the most relevant tools types (bifaces, cleavers, side-scrapers) we are also impelled to consider the occurrence of local evolutionary chronological trends. More data is still needed, however, not only to narrowly establish the age of each site, but also to relate this local sequence to others, at the regional level. This will hopefully allow the development of a new and more complete technological framework.

Acknowledgements

This study was supported by the Fundação para a Ciência e a Tecnologia, through projects PTDC/GEO-GEO/2860/2012 (FASTLOAD), UID/MAR/04292/2013 – MARE and UID/GEO/04683/2013 – ICT. The authors wish to thank David Bridgland and an anonymous reviewer for the very constructive comments and suggestions that greatly improved the manuscript.

References

Aslan, A., Autin, W.J., 1998. Holocene flood-plain soil formation in the southern lower Mississippi Valley: implications for interpreting alluvial paleosols. Bulletin of the Geological Society of America, 110, 433-449.

Barbosa, B.P., 1995. Alostratigrafia e Litostratigrafia das unidades continentais da Bacia Terciária do Baixo Tejo. Relações com o eustatismo e a tectónica. PhD Thesis, Univ. Lisboa, 253 p.

Bensaúde, A., 1910. Le tremblement de terre de la vallée du Tage du 23 avril 1909 (Note préliminaire). Bull. Soc. Port. Sc. Nat. III, 89-129.

779 Besana-Ostman, G.M., Villanova, S.P., Nemser, E.S., Falcão Flor, A.P., Heleno, S., Ferreira, H.,
780 Fonseca, J.D., 2012. Large Holocene Earthquakes in the Lower Tagus Valley Fault Zone,
781 Central Portugal. Seismological Research Letters 83 (1), 67-76, doi: 10.1785/gssrl.83.1.67.

782 Blum, M.D., Törnqvist, T.E., 2000. Fluvial responses to climate and sea-level change; a review and
783 look forward. Sedimentology 47 (Suppl. 1), 2-48.

784 Breuil, H., Zbyszewski, G., 1942. Contribution à l'étude des industries Paléolithiques du Portugal
785 et de leurs rapports avec la géologie du Quaternaire. Les principaux gisements des deux rivers
786 de l'ancien estuaire du Tage. Comunicações dos Serviços Geológicos de Portugal XXIII,
787 Lisboa, 369 p.

788 Breuil, H., Zbyszewski, G., 1945. Contribution à l´étude des industries Paléolithiques du Portugal
789 et de leurs rapports avec la géologie du Quaternaire. Les principaux gisements des plages
790 quaternaires du littoral d´Estremadura et des terrasses fluviales de la basse vallée du Tage.
791 Comunicações dos Serviços Geológicos de Portugal XXVI, Lisboa, 662 p.

792 Bridgland, D.R., Westaway, R., 2008. Climatically controlled river terrace staircases: a worldwide
793 Quaternary phenomenon. Geomorphology 98, 285-315.

794 Bridgland, D.R., Westaway, R., 2014. Quaternary fluvial archives and landscape evolution: a global
795 synthesis. Proceedings of the Geologists' Association 125, 600-629.

796 Bridgland, D.R., White, M.J., 2014. Fluvial archives as a framework for the Lower and Middle
797 Palaeolithic: patterns of British artefact distribution and potential chronological implications.
798 Boreas 43, 543-555.

799 Bridgland, D.R., White, M.J., 2015. Chronological variations in handaxes: patterns detected from
800 fluvial archives in NW Europe. Journal of Quaternary Science 30, 623-638.

801 Bridgland, D.R., Antoine, P., Limondin-Lozouet, N., Santisteban, J.I., Westaway, R., White, M.J.,
802 2006. The Palaeolithic occupation of Europe as revealed by evidence from the rivers: data
803 from IGCP 449. Journal of Quaternary Science 21, 437-455.

804 Bull, W.B., 2009. Geomorphic Responses to Climatic Change. Blackburn Press, 328 p.

805 Buylaert, J.P., Murray, A. S., Thomsen, K.J., Jain, M., 2009. Testing the potential of an elevated
806 temperature IRSL signal from K-feldspar. Radiation Measurments 44, 560-565.

807 Buylaert, J.-P., Jain, M., Murray, A.S., Thomsen, K.J., Thiel, C., Sohbati, R., 2012. A robust
808 feldspar luminescence dating method for Middle and Late Pleistocene sediments. Boreas 41,
809 435–451.

810 Buylaert, J.-P., Murray, A.S., Gebhardt, A.C., Sohbati, R., Ohlendorf, C., Thiel, C., Wastegård, S.,
811 Zolitschka, B., The PASADO Science Team, 2013. Luminescence dating of the PASADO core

812 5022-1D from Laguna Potrok Aike (Argentina) using IRSL signals from feldspar. Quaternary
813 Science Reviews 71, 70-80.

814 Cabral, J., 1995. Neotectónica de Portugal continental. Memórias do Instituto Geológico e Mineiro
815 Portugal 31, 265 p.

816 Cabral, J., 2012. Neotectonics of mainland Portugal: state of the art and future perspectives. Journal
817 of Iberian Geology 38 (1), 71-84.

818 Cabral, J., Ribeiro, A., 1988. Carta Neotectónica de Portugal Continental, Escala 1:1.000.000, Serv.
819 Geol. de Portugal, Lisboa.

820 Cabral, J., Ribeiro, A., 1989. Carta Neotectónica de Portugal Continental, Escala 1:1.000.000. Nota
821 explicativa. Serv. Geol. Portugal, Lisboa, 10 p.

822 Cabral, J.; Moniz, C.; Ribeiro, P.; Terrinha, P., Matias, L., 2003. Analysis of seismic reflection data
823 as a tool for the seismotectonic assessment of a low activity intraplate basin - the Lower Tagus
824 Valley (Portugal). Journal of Seismology 7, 431-447. doi: 10.1023/B:
825 JOSE.0000005722.23106.8d.

826 Cabral, J., Ribeiro, P., Figueiredo, P., Pimentel, N., Martins, A., 2004. The Azambuja fault: an
827 active structure located in an intraplate basin with significant seismicity (Lower Tagus Valley,
828 Portugal). J. Seismol. 8, 347–362.

829 Cabral, J. Moniz, C., Batló, J., Figueiredo, P., Carvalho, J., Matias, L., Teves-Costa, P., Dias, R.,
830 Simão, N., 2013. The 1909 Benavente (Portugal) earthquake: search for the source. Natural
831 Hazards, 69, 1211-1227. DOI 10.1007/s11069-011-0062-8.

832 Carvalho, J., Rabeh, T., Cabral, J., Carrilho, F., Miranda, J.M., 2008. Geophysical characterization
833 of the Ota–Vila Franca de Xira–Lisbon–Sesimbra fault zone, Portugal. Geophys. J. Int. 174,
834 567-584. doi: 10.1111/j.1365-246X.2008.03791.x.

835 Carvalho, J., Rabeh, T., Dias, R., Dias, R., Pinto, C., Oliveira, T., Cunha, T., Borges, J., 2014.
836 Tectonic and neotectonic implications of a new basement map of the Lower Tagus Valley,
837 Portugal. Tectonophysics 617, 88-100.

838 Chauhan, P., Bridgland, D., Moncel, M.-H., Antoine, P., Bahain, J.-J., Briant, R., Cunha, P.P.,
839 Locht, J.-L., Martins, A., Schreve, D., Shaw, A., Voinchet, P., Westaway, R., White, M., White,
840 T., *in press*. Fluvial deposits as an archive of early human activity: progress during the 20
841 years of the Fluvial Archives Group. Quaternary Science Reviews, Special Issue - Fluvial
842 Archives Group, JQSR-D-16-00195.

843 Choffat, P. 1907. Notice sur la Carte Hypsométrique du Portugal. Com. Serv. Geol. Portugal VII: 1-
844 71.

Corral, I., 1998a. Depositos Cuaternarios en el área de Constância-Barquinha-Entroncamento y la Rib. del Bezelga. In: Cruz, A.R., Oosterbeek, L., Reis, R.P. (Eds.), Arkeos 4, Quaternário e Pré-História do Alto Ribatejo (Portugal), CEIPHAR, 59-144.

Corral, I., 1998b. Secciones com material arqueológico en estrato en las proximidades de Atalaia. In: Cruz, A.R., Oosterbeek, L., Reis, R.P. (Eds.), Arkeos 4, Quaternário e Pré-História do Alto Ribatejo (Portugal), CEIPHAR, 227-250.

Cunha, P.P., 1992. Estratigrafia e sedimentologia dos depósitos do Cretácico Superior e Terciário de Portugal Central, a leste de Coimbra. PhD thesis, Univ. Coimbra, Portugal. 262 pp.

Cunha, P.P., 1996. Unidades litostratigráficas do Terciário da Beira Baixa (Portugal). Comum. Instituto Geol. Mineiro 82: 87-130.

Cunha, P.P., Barbosa, B.P., Pena dos Reis, R., 1993. Synthesis of the Piacenzian onshore record, between the Aveiro and Setúbal parallels (Western Portuguese margin). Ciências da Terra (Univ. Nova de Lisboa) 12, 35-43.

Cunha, P.P., Martins, A.A., Daveau, S., Friend, P.F., 2005. Tectonic control of the Tejo river fluvial incision during the late Cenozoic, in Ródão – central Portugal (Atlantic Iberian border). Geomorphology 64, 271-298.

Cunha, P. P., Martins, A.A., Huot, S., Murray, A., Raposo, L., 2008. Dating the Tejo River lower terraces in the Ródão area (Portugal) to assess the role of tectonics and uplift. Geomorphology 102, 43-54.

Cunha, P.P., Almeida, N.A.C., Aubry, T.; Martins, A.A.; Murray, A.S.; Buylaert, J.-P.; Sohbati, R., Raposo, L., Rocha, L., 2012. Records of human occupation from Pleistocene river terrace and aeolian sediments in the Arneiro depression (Lower Tejo River, central eastern Portugal). Geomorphology 165-166, 78-90.

Cunha, P.P., Martins, A.A., Gouveia, M.P., 2016. The terrace staircases of the Lower Tagus River (Ródão to Chamusca) – characterization and interpretation of the sedimentary, tectonic, climatic and and Palaeolithic data. Quaternary Studies 14, 1-24. http://www.apeq.pt/ojs/index.php/apeq.

De Vicente, G., Cloetingh, S., Van Wees, J.D., Cunha, P.P., 2011. Tectonic classification of Cenozoic Iberian foreland basins. Tectonophysics 502 (1-2), 38-61. doi:10.1016/j.tecto.2011.02.007

Dinka, T.M., Morgan, C.L.S, McInnes, K.J., Kishné, A.S., Harmel, R.D., 2013. Shrink–swell behavior of soil across a Vertisol catena. Journal of Hydrology 476, 352–359.

877 Diniz, F., Silva, C.M., Cachão, M. 2016. O Pliocénico de Pombal (Bacia do Mondego, Portugal
878 oeste): Biostratigrafia, Paleoecologia e Paleobiogeografia. Quaternary Studies 14, 41-59.
879 http://www.apeq.pt/ojs/index.php/apeq.

880 Douglass, J., Schmeeckle, M., 2007. Analogue modeling of transverse drainage mechanisms.
881 Geomorphology 84, 1-2, 22-43. http://dx.doi.org/10.1016/j.geomorph.2006.06.004

882 Duller, G.A.T., 2004. Luminescence dating of Quaternary sediments: recent advances. Journal of
883 Quaternary Science 19, 183–192.

884 Freire de Andrade, C.B., 1933. A tectónica do estuário do Tejo e dos vales submarinos ao largo da
885 costa da Caparica, e sua relação com as nascentes termo-medicinais de Lisboa. Com. Serv.
886 Geol. Portugal 19, 23-40.

887 Gibbard, P.L., Lewin, J., 2002. Climate and related controls on interglacial sedimentation in
888 lowland Britan. Sedimentary Geology 151, 187-210.

889 Huggett, R.J., 1998. Soil chronosequences, soil development, and soil evolution: a critical review.
890 Catena 32, 155–172.

891 Huntley, D.J., Baril, M.R., 1997. The K content of the K-feldspars being measured in optical dating
892 or in thermoluminescence dating. Ancient TL 15, 11–13.

893 Jahn, R., Blume, H.P., Asio, V.B., Spaargaren, O., Schad, P., Langohr, R., Brinkman, R.,
894 Nachtergaele, F.O., Pavel Krasilnikov, R., 2006. Guidelines for soil description. FAO, Rome,
895 97 p.

896 Lamothe, M., Auclair, M., Hamzaoui, C., Huot, S., 2003. Towards a prediction of long-term
897 anomalous fading of feldspar IRSL. Radiation Measurements 37, 493-498.

898 Lewis, S., Maddy, D., Glenday, S., 2004. The Thames Valley Sediment Conveyor: fluvial system
899 development over the last two interglacial–glacial cycles. Quaternaire 15, 17–28.

900 Lisiecki, L.E., Raymo, M.E., 2005. A Pliocene-Pleistocene stack of 57 globally distributed benthic
901 δ18O records. Paleoceanography 20 (1), 1-17: Doi 10.1029/2004PA001071

902 López-Recio, M., Silva, P.G., Cunha, P.P., Tapias, F., Roquero, E., Morín, J., Carrobles, J., Murray,
903 A.S., Buylaert, J.-P., 2013. Dataciones por luminiscencia de la terraza +25-30 m del río Tajo
904 en la área de Toledo. El yacimiento Achelense de Pinedo. Proceedings VIII Reunión de
905 Cuaternario Ibérico, 17-21.

906 López-Recio, M., Silva, P.G.; Roquero, E., Cunha, P.P., Tapias, F., Alcaraz-Castaño, M., Baena, J.,
907 Cuartero, F., Morín, J., Torres, T., Ortiz, J.E., Murray, A.S., Buylaert, J.P., 2015. Geocrolología
908 de los yacimientos achelenses de Pinedo y Cien Fanegas (Valle del Tajo) e implicaciones en la
909 evolución fluvial en el entorno de Toledo (España). Estudios Geológicos 71 (1), 1-19.

910 Martins, A.A., 1999. Caracterização morfotectónica e morfossedimentar da Bacia do Baixo Tejo
911 (Pliocénico e Quaternário). PhD Thesis, University of Évora, 500 p.

912 Martins, A.A., Cunha, P.P., Huot, S., Murray, A., Buylaert, J.-P., 2009. Geomorphological
913 correlation of the tectonically displaced Tejo river terraces (Gavião-Chamusca area, Portugal)
914 supported by luminescence dating. Quaternary International 199, 75-91.

915 Martins, A.A., Cunha, P.P., Buylaert, J.-P., Huot, S., Murray, A., Dinis, P., Stokes, M., 2010a. K-
916 feldspar IRSL dating of a Pleistocene river terrace sequence of the Lower Tejo River
917 (Portugal, western Iberia). Quaternary Geochronology 5, 176-180.

918 Martins, A.A., Cunha, P.P., Rosina, P., Osterbeek, L., Cura, S., Grimaldi, S., Gomes, J., Buylaert,
919 J.-P., Murray, A., Matos, J., 2010b. Geoarchaeology of Pleistocene open-air sites in the Vila
920 Nova da Barquinha-Santa Cita area (Lower Tejo River basin, central Portugal). Proceedings of
921 the Geologists' Association 121, 128-140.

922 Merritts, J., Vicent, R., Wohl, E., 1994. Long river profiles, tectonism and eustasy: a guide to
923 interpreting fluvial terraces. Journal of Geophysical Research 99, B7, 14031-14050.

924 Montenegro de Andrade, M., 1944. Estudo polínico de algumas formações turfo-linhitosas
925 portuguesas. Publicações do Museu e Laboratório de Mineralogia e Geologia da Faculdade de
926 Ciências do Porto 37, 5-11.

927 Mozzi, P., Azevedo, T., Nunes, E., Raposo, L., 2000. Middle terrace deposits of the Tagus river in
928 Alpiarça, Portugal, in relation to early human occupation. Quaternary Research 54, 359-371.

929 Murray A.S., Wintle A.G., 2000. Luminescence dating of quartz using an improved single-aliquot
930 regenerative-dose protocol. Radiation Measurements 32, 57-73.

931 Murray, A.S., Wintle, A.G., 2003. The single aliquot regenerative dose protocol: potential for
932 improvements in reliability. Radiation Measurements 37, 377-381.

933 Murray, A., Marten, R., Johnston, A., Martin, P., 1987. Analysis for naturally occurring
934 radionuclides at environmental concentrations by gamma spectrometry. Journal of
935 Radioanalytical and Nuclear Chemistry 115, 263-288.

936 Murray, A.S., Thomsen, K.J., Masuda, N., Buylaert, J.-P., Jain, M., 2012. Identifying well-bleached
937 quartz using the different bleaching rates of quartz and feldspar luminescence signals. Radia-
938 tion Measurements 47, 688-695.

939 Murray-Wallace, C.V., Woodroffe, C.D., 2014. Quaternary Sea-Level Changes: A Global Perspec-
940 tive. Cambridge University Press, Cambridge, UK, 502 p.

941 Oliveira, J.T., Pereira, E., Ramalho, M., Antunes, M.T., Monteiro, J.H. (Coord.), 1992. Carta
942 Geológica de Portugal à escala 1/500000, 5.ª edição, Serviços Geológicos de Portugal, Lisboa.

943 Olley, J.M., Murray, A.S., Roberts, R.G., 1996. The effects of disequilibria in the uranium and
944 thorium decay chains on burial dose rates in fluvial sediments. Quaternary Science Reviews
945 15, 751–760.

946 Pais, J., Cunha, P.P., Pereira, D., Legoinha, P., Dias, R., Moura, D., Brum da Silveira, A., Kullberg,
947 J.C., González-Delgado, J.A., 2012. The Paleogene and Neogene of Western Iberia (Portugal).
948 A Cenozoic record in the European Atlantic domain. SpringerBriefs in Earth Sciences,
949 Springer, Series ID: 8897, 158 p.

950 Pal, D.K., Bhattacharyya, T., Chandran, P., Ray, S.K., Satyavathi, P.L.A., Durge, S.L., Raja, P.,
951 Maurya, U.K., 2009. Vertisols (cracking clay soils) in a climosequence of Peninsular India:
952 Evidence for Holocene climate changes. Quaternary International 209, 6–21.

953 Panera, J., Rubio-Jara, S., Yravedra, J., Hugues-Alexandre, B., Sesé, C., Pérez-González, A., 2014.
954 Manzanares Valley (Madrid, Spain): a good country for Proboscideans and Neanderthals.
955 Quaternary International 326-327, 329-343.

956 Pérez-González A. 1994. Depresión del Tajo. In: Gutiérrez-Elorza, M. (Ed.), Geomorfologia de
957 España. Editorial Rueda, 389-436.

958 Pérez-González, A., Gallardo-Millán, J.L., Uribelarrea del Val, D., Panera, J., Rubio-Jara, S., 2013.
959 La inversión Matuyama-Brunhes en la secuencia de terrazas del río Jarama entre Velilla de
960 San Antonio y Altos de la Mejorada, al SE de Madrid (España). Estudios Geológicos 69 (1),
961 35-46.

962 Ramos, A., Cunha, P.P., Cunha, L., Gomes, A., Lopes, F.C, Buylaert, J.-P., Murray, A.S., 2012.
963 The River Mondego terraces at the Figueira da Foz coastal area (western central Portugal):
964 geomorphological and sedimentological characterization of a terrace staircase affected by
965 differential uplift and glacio-eustasy. Geomorphology 165-166, 107-123.

966 Raposo, L., 1995a. Ambientes, territórios y subsistência en el Paleolítico Médio de Portugal.
967 Complutum 6, 57-77.

968 Raposo, L., 1995b. O Paleolítico. In: Medina, J. (Ed.), História de Portugal, vol. 1. Clube
969 Internacional do Livro, 23–85.

970 Raposo, L., 1996. Quartzite bifaces and cleavers in the final Acheulian assemblages of Milharós
971 (Alpiarça, Portugal). In: Non-Flint Stone Tools and Palaeolithic Occupation of the Iberian
972 Península, Edt. N. Moloney, L. Raposo, M. Santajoa. Tempvs Reparatvm, Bar International
973 Series 649, 151-165.

974 Raposo, L., 2002. Um século de estudos no Paleolítico Médio em Portugal: balanço e perspectivas.
975 Arqueologia e História 54, 25-39.

Raposo. L., Cardoso, J.L., 1998. O sítio do Paleolítico Médio da Conceição, Alcochete. Centro de Estudos e Monitorização Ambiental – CEMA, 74 pp.

Raposo, L., Carreira, J.R., Salvador, M., 1985. A estação Acheulense final de Milharós, Vale do Forno, Alpiarça. Proceedings of I Reunião do Quaternário Ibérico, vol. 2, 41-60.

Roe, D.A., 1968. British Lower and Middle Palaeolithic hand axe groups. Proceedings of the Prehistoric Society 34, 1-82.

Roquero, E., Silva, P.G., Zazo, C., Goy, J.L., Masana, J., 2015a. Soil evolution indices in fluvial 896 terrace chronosequences of Central Spain (Tagus and Duero fluvial basins). Quaternary International 376, 101-113.

Roquero, E., Silva, P.G., López Recio, M., Tapias, F., Cunha, P.P., Morín, J., Alcaraz-Castaño, M., Carrobles, J., Murray, A.S., Buylaert, J.P., 2015b. Geocronología de las terrazas de Pleistoceno Medio y Superior del valle del Tajo en Toledo (España). In: Una vision global del Cuaternario. El hombre como condicionante de processos geológicos (J.P. Galve, J.M. Azañon, J.V. Pérez Peña y P. Ruano, Eds.), pp. 8-12. XIV Reunión Nacional de Cuaternario, Granada.

Rosina, P., 2002. Stratigraphie et géomorphologie des terrasses fluviatiles de la moyenne Vallée du Tage (Haut Ribatejo, Portugal). In: Cruz, A.R., Oosterbeek, L. (Eds.), Arkeos 13, Territórios, mobilidade e povoamento no Alto-Ribatejo. IV: Contextos macrolíticos. CEIPHAR, 11-52.

Rosina, P., Voinchet, P., Bahain, J., Cristovão, J., Falguères, C., 2014. Dating the onset of Lower Tagus River terrace formation using electron spin resonance. Journal of Quaternary Science 29(2), 153-162.

Roucoux, K.H., de Abreu, L., Shackleton, N.J., Tzedakis, P.C., 2005. The response of NW Iberian vegetation to North Atlantic climate oscillations during the last 65 kyr. Quaternary Science Review 24, 1637-1653.

Roucoux, K., Tzedakis, P., de Abreu, L., Shackleton, N., 2006. Climate and vegetation changes 180,000 to 345,000 years ago recorded in a deep-sea core off Portugal. Earth and Planetary Science Letters 249, 307-325.

Rubio-Jara, S., Panera, J., Rodríguez de Tembleque, J., Santonja, M., Pérez-González, A., 2016 Large flake Acheulean in the middle of Tagus basin (Spain): Middle stretch of the river Tagus valley 914 and lower stretches of the rivers Jarama and Manzanares valleys. Quaternary international, http://dx.doi.org/10.1016/j.quaint.2015.12.023

Salgueiro, E., Voelker, A.H.L., Abreu, L. de, Abrantes, F., Meggers, H., Wefer, G., 2010. Temperature and productivity changes off the western Iberian margin during the last 150 ky. Quaternary Science Reviews 29, 680-695.

Santonja, M., Villa, P., 2006. The Acheulian of Western Europe. In: Goren-Inbar, N., Sharon, G. (Eds.), Axe Age: Acheulian Tool-making from Quarry to Discard. Approaches to Anthropological Archaeology Series. Equinox Publishing, 608 p.

Santonja, M., Pérez-González, A., 2010. Mid-Pleistocene Acheulian industrial complex in the Iberian Peninsula. Quaternary International 223-224, 154-161.

Silva, P.G., Roquero, E., López-Recio, M., Huerta, P., Martínez-Graña, A.M., 2016, in press. Chronology of fluvial terrace sequences for large Atlantic rivers in the Iberian Peninsula (Upper Tagus and Duero drainage basins, Central Spain). Quaternary Science Reviews, http://dx.doi.org/10.1016/j.quascirev.2016.05.027

Stokes, M., Cunha, P.P., Martins, A.A., 2012. Techniques for analysing river terrace sequences. Geomorphology 165-166, 1-6. Doi: 10.1016/j.geomorph.2012.03.022

Thomsen, K.J., Murray, A.S., Jain, M., Bøtter-Jensen, L., 2008. Laboratory fading rates of various luminescence signals from feldspar-rich sediment extracts. Radiation Measurements 43, 1474-1486.

Van der Schriek, T., Passmore, D.G., Rolão, J., Stevenson, A.C., 2007. Estuarine–fluvial floodplain formation in the Holocene Lower Tagus valley (Central Portugal) and implications for Quaternary fluvial system evolution. Quaternary Science Reviews 26, 2937-2957.

Vilanova, S.P., Fonseca, J.F.B.D. 2004. Seismic hazard impact of the Lower Tagus Valley Fault Zone (SW Iberia). Journal of Seismology 8, 331-345.

Vis, G.-J., 2009. Fluvial and Marine sedimentation at a passive continental margin. The late Quaternary Tagus depositional system. PhD thesis, Vrije University, 244 p.

Vis, G.-J., Kasse, C., Vandenberghe, J., 2008. Late Pleistocene and Holocene palaeogeography of the Lower Tagus Valley (Portugal): effects of relative sea level, valley morphology and sediment supply. Quaternary Science Reviews 27, 1682–1709.

Vis, G.-J., Kasse, C., Kroon, D., Vandenberghe, J., Jung, S., Lebreiro, S.M., Rodrigues, T., 2016. Time-integrated 3D approach of late Quaternary sediment-depocenter migration in the Tagus depositional systems: From river valley to abyssal plain. Earth-Science Reviews 153, 192-211.

Yaalon, D.H., 1983. Climate, time and soil development. In: Wilding, L.P., Smeck, N.E., Hall, G.F. (Eds.), Pedogenesis and Soil Taxonomy: I. Concepts and Interactions. Elsevier, Amsterdam, 223–251.

Vepraskas, M.J., Lindbo, D.L., 2012. Redoximorphic features as related to soil hydrology and hydric Soils. Hydropedology, 143-172.

White, T.S., Bridgland, D.R., Westaway, R., Straw, A., in press. Evidence for late Middle Pleistocene glaciation of the British margin of the southern North Sea. Journal of Quaternary Science.

Wintle, A.G., Murray, A.S., 2006. A review of quartz optically stimulated luminescence characteristics and their relevance in single-aliquot regeneration dating protocols. Radiation Measurements 41, 369-391.

Wright, J.D., 2000. Global climate change in Marine Stable Isotope Records. In: Stratton Noler, J., Sowers, J.M. and Lettis, W.R. (Eds.), Quaternary Geochronology. Methods and applications, 427-433.

Zbyszewski, G., 1943. La classification du Paléolithic ancien et la chronologie du Quaternaire de Portugal en 1942. Boletim da Sociedade Geológica de Portugal 2, 2-3, 111 p.

Zbyszewski, G., 1946. Étude géologique de la region d'Alpiarça. Comunicações dos Serviços Geológicos de Portugal XXVII, 145-268.

Zbyszewski, G., 1977. Três ossos de vertebrados quaternários. Comunicações dos Serviços Geológicos de Portugal LXII, 191-194.

Zielhofer, C., Recio Espejo, J.M., Nunez Granados, M.A., Faust, D., 2009. Durations of soil formation and soil development indices in a Holocene Mediterranean floodplain. Quaternary International 209, 44-65.

Figure captions

Fig. 1. Location of the study area in the Lower Tejo (central Portugal). Hipsometry and digital elevation model obtained from SRTM data.

Fig. 2. Simplified geological map of the region (adapted from the Carta Geológica de Portugal, 1/500,000, Oliveira et al., 1992 and Barbosa, 1995). 1 – metasediments of the Hesperian Massif; 2 – granites of the Hesperian Massif; 3 – limestones and sandstones (Mesozoic); 4 – sandstones and conglomerates (Palaeogene); 5 – sands (Lower Miocene); 6 – silts and clays (Miocene); 7 – limestones, silts and clays (Miocene); 8 – gravels and sands (Pliocene); 9 – gravels of fluvial terraces (Pleistocene); 10 – modern alluvium: mud, silt and sand (Holocene); 11 – thrust fault; 12 - fault; 13 - stream; 14 – archaeological site.

Fig. 3. Terrace staircase of the River Tejo reach IV. The T6 terrace is only visible near Azinhaga village, whilst T5 is buried by modern alluvium downstream of Muge. Note the asymmetric development of the terraces between the two sides of Tejo valley downstream of Chamusca. Terraces are very scarce on the west side of the river valley.

Fig. 4. Map of the Alpiarça area, comprising the River Tejo tributary valleys of Vale do Forno and Vale de Atela. Location of the sites and cross sections (A – Á and B – B´). It is deduced from the contour lines that the interfluves between the Vale do Forno and Vale de Atela is developed in eroded (dissected) uppermost T4 deposits.

Fig. 5. Stratigraphic cross section A – Á. See Fig. 4 for location of the cross section and location of the OSL samples AM 21 and Atela 3.

Fig. 6. Stratigraphic cross section B – B´. This section shows that the US unit is dominated by sand channel facies in the west and rich in flood-plain clayish silts in the east. The topographic position of sample AM 15 is at near distance from the cross section (see Fig. 4), in the west side of the Vale do Forno streamlet.

Fig. 7. Stratigraphic logs of the sections at V. Forno (the VF8 site), V.Atela–W and V.Atela–E (see Fig. 4 for location). Most of the samples for luminescence dating are from here (AM 15, VForno 8-2, VForno 8-7, VForno 1,VForno 2, Atela 2, Atela 3 and Atela 4). 1 – archaeological level; 2 – vegetal macro remains; 3 – coal fragment; 4 – channel geometry; 5 – fossil roots; 6 – Maximum pebble size (mean diameter of the larger 10 clasts per level); 7 – sample for luminescence dating; 8 – sample for sedimentology; 9 – paleocurrent derived from planar cross-bedding.

Fig. 8. The V.Atela-E outcrop, with the base at the transition of the LG unit to the US unit. Almost all of the local thickness of the US unit is exposed here (ca. 18 m). The Atela 2 sample was collected at ~2.5 m below the cliff top.

Fig. 9. Paleosols developed in the overbank deposits of the T4 terrace US unit, at the AL1 site.

Fig. 10. Large Acheulian cutting tools from VF1 site. 1 to 4 – Cleavers; 5 to 9 – Bifaces.

Fig 11. The Acheulian industry of VF8 site. Large cutting tools. 1 to 4 – Cleavers; 5 to 9 – Bifaces.

Fig 12. The Acheulian industry of VF8 site. Flake tools. 1 to 6 – Denticulates and notches; 7 to 10 – Sidescrapers; 11 to 20 – Borers; 21 and 22 – Scrapers on ventral face.

Fig. 13. The final Achdeulian industry of VF3 site (Milharós site). Bifacial tools. 1 to 5 – Bifaces (Micoquian, lanceolate, ovalar); 6 and 7 – Bifaces with distal cutting edge.

Fig.14. The final Achdeulian industry of VF3 site (Milharós site)**.** Large cutting tools on primary Acheulian flakes and cores. 1 to 3 – Cleavers; 4 – Chopper on probably broken cleaver; 5 – Sidescraper; 6 – Bypiramidal core; 7 – Proto-*Levallois* core.

Fig. 15. a) First IR stimulation plateau for sample 102226. The natural signals are expressed as a fraction of the saturation level of the dose response curve. Three aliquots were measured per temperature and error bars represent one standard error. The inset shows the sensitivity corrected natural pIRIR290 signal (horizontal solid line) interpolated on the dose response curve for one aliquot measured using a first IR stimulation temperature of 50°C. b) Results of the dose recovery measurements. At least three aliquots were measured per data point and error bars represent one standard error. c) IR50 De values plotted as a function of the pIRIR290 De values for samples for which the pIRIR290 De is ≤ 2xD0 (see Table 4); error bars represent one standard error. The dashed line is the best fit through the data points.

Fig. 16. Map of the Tejo terrace staircase in the Muge area, downstream of Alpiarça. Stratigraphic location of the samples collected for luminescence dating: AM-22 (T4, base of the US unit); PSabug-2 (T5 top); Muge-1 and Muge-2 (T5 top); Almer-1 (Carregueira Formation; aeolian cover sands, not mapped in this figure).

Fig. 17. Burial ages of samples collected from Middle to Late Pleistocene sedimentary units of the Tejo reach IV, plotted according to the respective elevation a.r.b. (right axis).

Horizontal bars indicate the dominant lithologies for the fluvial deposits (black – gravels; blue – sands; green – silty clays) and the probable age range of each sedimentary unit. For this reach, the periods of aggradation are represented by green line segments and the periods of river downcutting are represented by red line segments that cross the sea-level curve (scaled benthic isotopes from V19-30, after Cutler et al., 2003), testifying a dominant sedimentary control by glacio-eustasy. T3, T4, T5 and T6 – terraces; CS – Carregueira Formation (aeolian sands); AP – Alluvial plain deposits. MIS intervals are according to Lisiecki and Raymo (2005). ESR – Electron Spin Ressonance age; pIRIR – post-IR $IRSL_{290}$ SAR age (m – minimum age); IRSL – $IRSL_{50}$ SAR age (m – minimum age); Qz-OSL – Quartz OSL SAR age.

Table captions

Table 1

Summary of the geomorphological and sedimentological characteristics of the sedimentary units present in the terrace staircase at Alpiarça. The main sites containing Palaeolithic industries located in the Lower Tejo reach IV are also listed. MPS – maximum pebble size (cm).

Table 2

The main features of palaeosols within the US unit.

Table 3

Burial depth, Radionuclide activities (^{238}U, ^{226}Ra, ^{232}Th and ^{40}K) and water content used for dose rate calculations of the luminescence dating samples.

Table 4

Summary of the luminescence ages obtained from sediment samples of the study area. All ages were obtained by using a post $IRIR_{290}$ protocol (K-feldspar; KF). For samples having natural $pIRIR_{290}$ signals >86% of the saturation level of the dose response curves, a minimum age is given based on the $2xD_0$ value. The doses used to calculate ages are highlighted in bold. The IR_{50} D_e values were obtained as part of the $pIRIR_{290}$ measurement

protocol. Samples 132201 (Almer-1), 102232 (PSabug-3) and 102263 (Ptmuge) were also measured using standard large aliquot quartz SAR-OSL (Q).

Table1

Table 1

Geomorphic unit, main site	Elevation above sea level and above river bed	Down-cutting from the previous geomorphic unit	Thickness of the associated deposits	Sedimentary characteristics of the associated sedimentary deposits	Main sites with lithic industries in stratigraphy
Culminant surface of the sedimentary basin (CSS)	152 m a.s.l. +144 m (a.r.b.)	0 m	35-40 m	Gravels with very coarse sands with through cross lamination. Clasts of quarzite (80%) and quartz (20%). MPS =15 cm	Not found
T1 terrace	115 m a.s.l. +107 m (a.r.b.)	42 m	5 m	Gravels with clasts of quarzite (76%) and quartz (26%). MPS = 22 cm	Not found
T2 terrace	82 m a.s.l. +74 m (a.r.b.)	40 m	6-7 m	Gravels with clasts of quarzite (69%) and quartz (31%). MPS = 17 cm	Not found
T3 terrace	60 m a.s.l. +52 m (a.r.b.)	32 m	10 m	Gravels with clasts of quarzite (56%) and quartz (44%). MPS = 22 cm	Not found
T4 terrace	38 m a.s.l. +30 m (a.r.b.)	52 m	25-30 m	Gravels with clasts of quarzite (68%) and quartz (32%). MPS=20cm. Sands and clays.	*Achaeulean*; Vale do Forno; Vale da Atela; Quinta da Boavista; Ribeira da Ponte da Pedra
T5 terrace (partially buried)	15 m a.s.l. +7 m (a.r.b.)	33 m	ca. 9-10 m m	Coarse to fine sands and clays	*Mousterian*; S. Antão do Tojal
T6 terrace (buried)	-4 m a.s.l. -12 m (a.r.b.)	ca. 37 m	ca. 18 m	Very coarse gravelly sands	*Late Mousterian*; Santa Cita
Alluvial plain	10 m a.s.l. +2 m (a.r.b.)	ca. 24 m	ca. 30 m	Silty clays and coarse to fine sands	*Mesolithic* and more recent industries (several sites)

Table2

Table 2

Horizon	Thickness (cm)	Grain size	Colour (Munsell)	Structure	Slickensides pressure faces	Lower boundary	Other features
Soil 3 (upper)							
A1	35	silty clay	10YR 5/2	very coarse platy from sedimentary laminae	common	clear smooth	-
Ai	40	silty clay	10YR	strong coarse prismatic	abundant	abrupt irregular	-
Bw	50	Silt	5Y 6/3	strong coarse prismatic	-	clear wavy	-
BCi	95	clayey silt	2.5Y 6/2	moderate coarse prismatic	common	gradual	transition to Ai hor. of soil 2
Soil 2 (middle)							
Ai	35	silty clay	10YR 5/3	strong coarse prismatic	abundant	clear wavy to irregular	-
Bw	60	Silt	2.5Y 5/4	strong coarse prismatic to angular blocky	-	gradual smooth	-
C1	70	sandy silt	2.5Y 6/4	massive	-	Gradual smooth	-
C2	20-40	silty coarse sand	2.5Y 6/4	massive	-	abrupt wavy	locally erosive on Ai hor. of soil 1
Soil 1 (lower)							
Ai	40	silty clay	10YR 5/3	strong coarse prismatic	Abundant	clear smooth	-
Bw	25	Silt	2.5Y 6/4	moderate coarse angular blocky	-	abrupt wavy	abundant bioturbation
Cm	55	Silt	2.5Y 6/4	weak coarse angular blocky to massive	-	unknown	1 cm-thick iron crust, abundant Fe-Mn nodules

Table 3

Sample code	Field code	Burial Depth (cm)	U-238 (Bq kg^{-1})	Ra-226 (Bq kg^{-1})	Th-232 (Bq kg^{-1})	K-40 (Bq kg^{-1})	Water content (%)
132201	*Almer 1*	80	12±4	17.4±0.4	22.8±0.5	808±14	5
072226	Azinh-3	60	49±8	34.1±0.7	46.5±0.8	853±17	15
102233	SATojal-1	1500	55±10	44.2±0.9	71.3±1.1	710±16	9
102272	Atojal-2	2500	18±3	21.2±0.3	32.9±0.4	368±8	25
102231	PSabug-2	145	41±6	40.2±0.7	61.3±0.8	875±19	18
PC5239	Muge-1	60	30±6	20.2±0.5	23.0±0.5	989±18	10
PC5240	Muge-2	100	14±3	14.0±0.3	18.3±0.3	806±14	11
132245	VForno-2	50	14±6	12.2±0.5	14.2±0.5	1022±20	5
132244	VForno-1	100	14±6	17.5±0.5	22.3±0.6	964±18	12
072257	VForno8-2	300	61±8	56.6±0.9	63.6±1.0	829±17	15
052216	AM-15	400	13±4	16.4±0.6	20.0±0.6	1054±21	22
052222	AM-21	275	24±6	19.9±1.0	24.6±0.9	800±29	26
052223	AM-22	375	20±4	19.6±0.5	14.3±0.4	873±15	22
132246	VCaval-1	500	17±7	21.2±0.6	32.6±0.7	1003±20	8
132202	Atela-2	250	26±6	25.4±0.5	30.4±0.6	907±17	11
132203	Atela-3	>1100	28±6	18.6±0.5	17.5±0.6	962±19	10
102226	VgPeso-1	700	18±7	13.8±0.5	21.8±0.6	798±16	10
102263	Ptmuge	30	21±3	24.5±0.3	28.8±0.4	1125±17	20
102232	Psabug-3	5	28±7	22.7±0.6	22.6±0.6	1104±21	28

Table4

Table 4

Site	NLL and field code	Altitude (m)	Lithology and Lithostratigraphic unit	IR_{50} D_e (Gy)	$pIRIR_{290}$ D_e (Gy)	$pIRIR_{290}$ 2*Do (Gy)	Dose rate (Gy/ka)	n	Age (ka)
Almeirim	132201 Almer-1	22	Aeolian medium sand Carregueira formation	42.6±1.5	**60.7 ± 1.9 (Q)** **81.6±1.7 (FK)**	-	3.18±0.14 (Q) 4.00±0.15 (FK)	12 (Q) 6 (FK)	19.1±1.1 (Q) 20.4±1.1 (FK)
Azinhaga	072226 Azinh-3	16.4	Pebbly coarse sand T6 (top)	102±7	**181±8**	-	4.64±0.16	18	39±2
Sto. Antão do Tojal	102233 SATojal-1	6.5	Medium sand T5 (top)	155±9	**399±10**	-	4.93±0.19	12	81±4
Sto. Antão do Tojal	102272 Atojal-2	5.5	Silty clay T5 (top)	104±11	**200±35**	-	2.66±0.10	6	75±14
Porto Sabugueiro	102231 PSabug-2	9.0	Coarse sand T5 (top)	170±11	**375±28**	-	5.03±0.18	6	75±6
Rib. Muge	PC5239 Muge-1	13	Medium to fine sand T5 (top)	259±16	**426 ±12**	846±66	4.57±0.20	9	93 ± 5
Rib. Muge	PC5240 Muge-2	12.6	Medium to fine sand T5 (top)	235±5	**355 ±13**	838±14	3.81±0.16	6	93 ± 5
Vale do Forno	132245 VForno-2	33.5	Medium sand T4 (US topmost)	410±20	**685 ±25**	861±14	4.44±0.20	3	154±10
Vale do Forno	132244 VForno-1	33	Medium sand T4 (US topmost)	370±30	**661 ±24**	1042±25	4.19±0.18	6	158±9
Vale do Forno	072257 VForno8-2	31	Fine sand T4 (US middle)	490±20	**1011±71**	1022±55	5.03±0.18	3	201±16
Vale do Forno	052216 AM-15	15	Coarse sand T4 (US base)	-	1130±90	**963±10**	3.64±0.13	3	>270
Quinta dos Patudos	052222 AM-21	34	Coarse sand T4 (US middle)	-	1330±270	**1048±45**	3.53±0.12	3	>300

Fonte da Burra	052223 *AM-22*	5.0	Coarse sand T4 (US base)	-	1180±50	**984±42**	3.64±0.12	3	>270
Vale de Cavalos	132246 *VCaval-1*	23	Medium sand T4 (US base)	-	1700±60	**926±15**	4.59±0.21	2	> 200
Vale de Atela	132202 *Atela-2*	33	Medium sand T4 (US top)	-	1170±70	**784±20**	4.29±0.18	3	>200
Vale de Atela	132203 *Atela-3*	19	Pebbly medium sand T4 (LG middle)	-	1500±290	**879±37**	4.00±0.18	3	>200
V. geodésico Peso	102226 Vg Peso 1	71	Gravelly coarse sand T1	-	1600±50	**1170±40**	3.85±0.14	3	>304
Porto de Muge	102263 Ptmuge	3.0	Medium sand Modern river bed	3.6±1.1	**0.81±0.14 (Q)** **15.36±1.02 (FK)**	-	3.85±0.15 (Q) 4.62±0.16 (FK)	12 (Q) 15 (FK)	0.21±0.04 (Q) 3.32±0.26 (FK)
Porto Sabugueiro	102232 PSabug-3	4.0	Coarse sand Modern river bed	2.7±0.3	**0.57±0.12 (Q)** **20.5±2.5 (FK)**	-	3.52±0.13 (Q) 4.24±0.14 (FK)	34 (Q) 6 (FK)	0.16±0.03 (Q) 4.83±0.63 (FK)

Figure1

Click here to download high resolution image

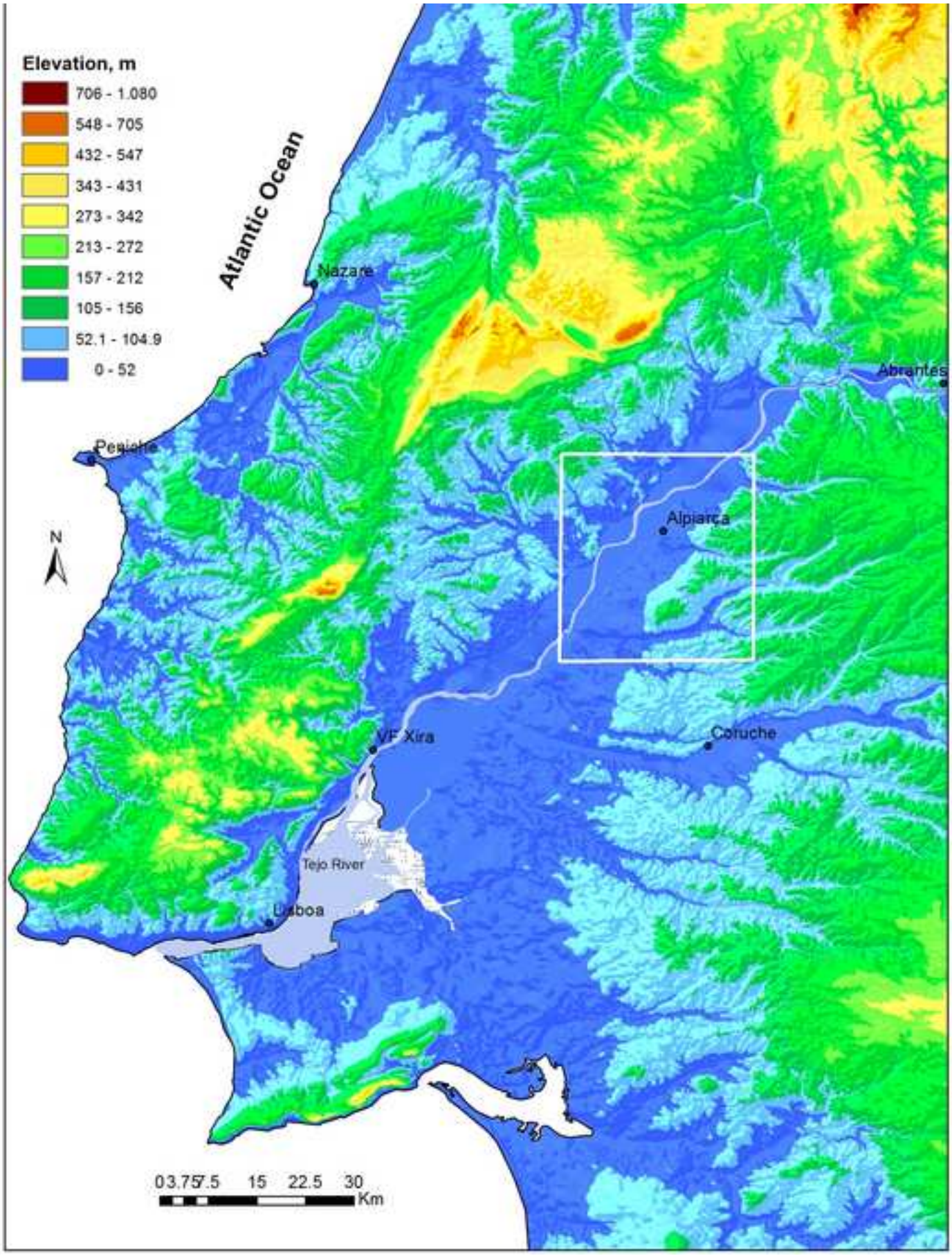

Figure2

Click here to download high resolution image

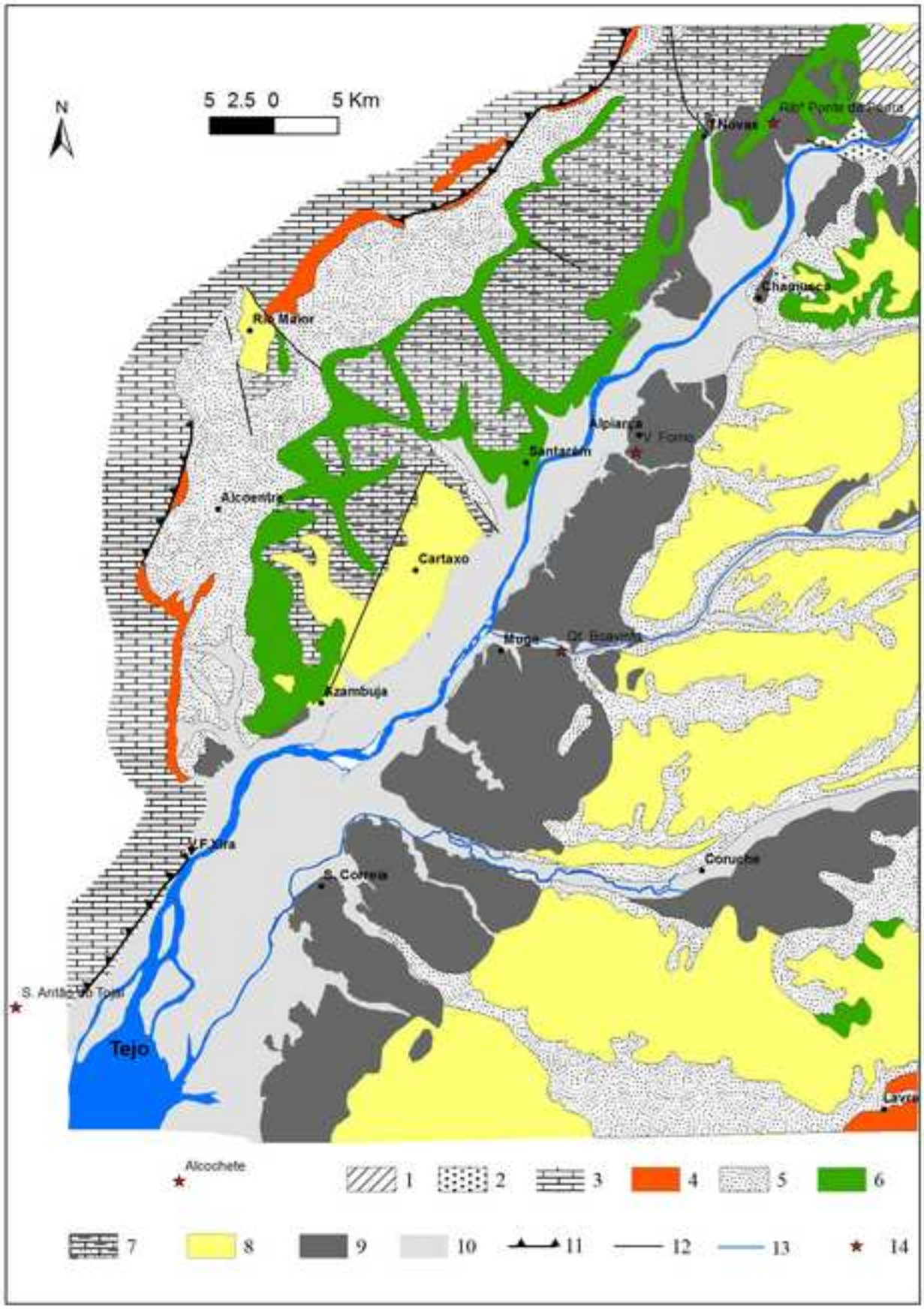

Figure3

Click here to download high resolution image

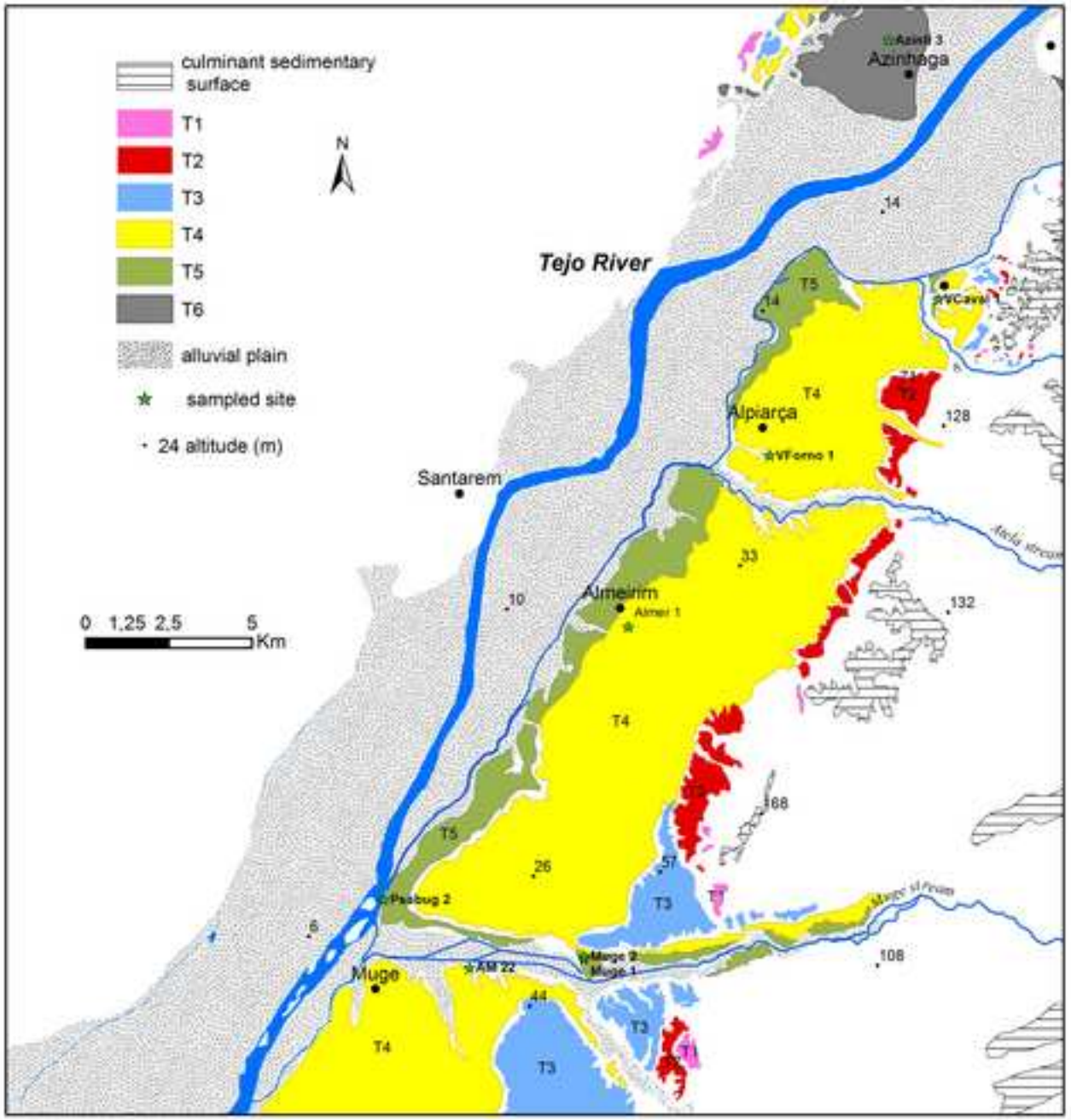

Figure4

Click here to download high resolution image

Figure5

Click here to download high resolution image

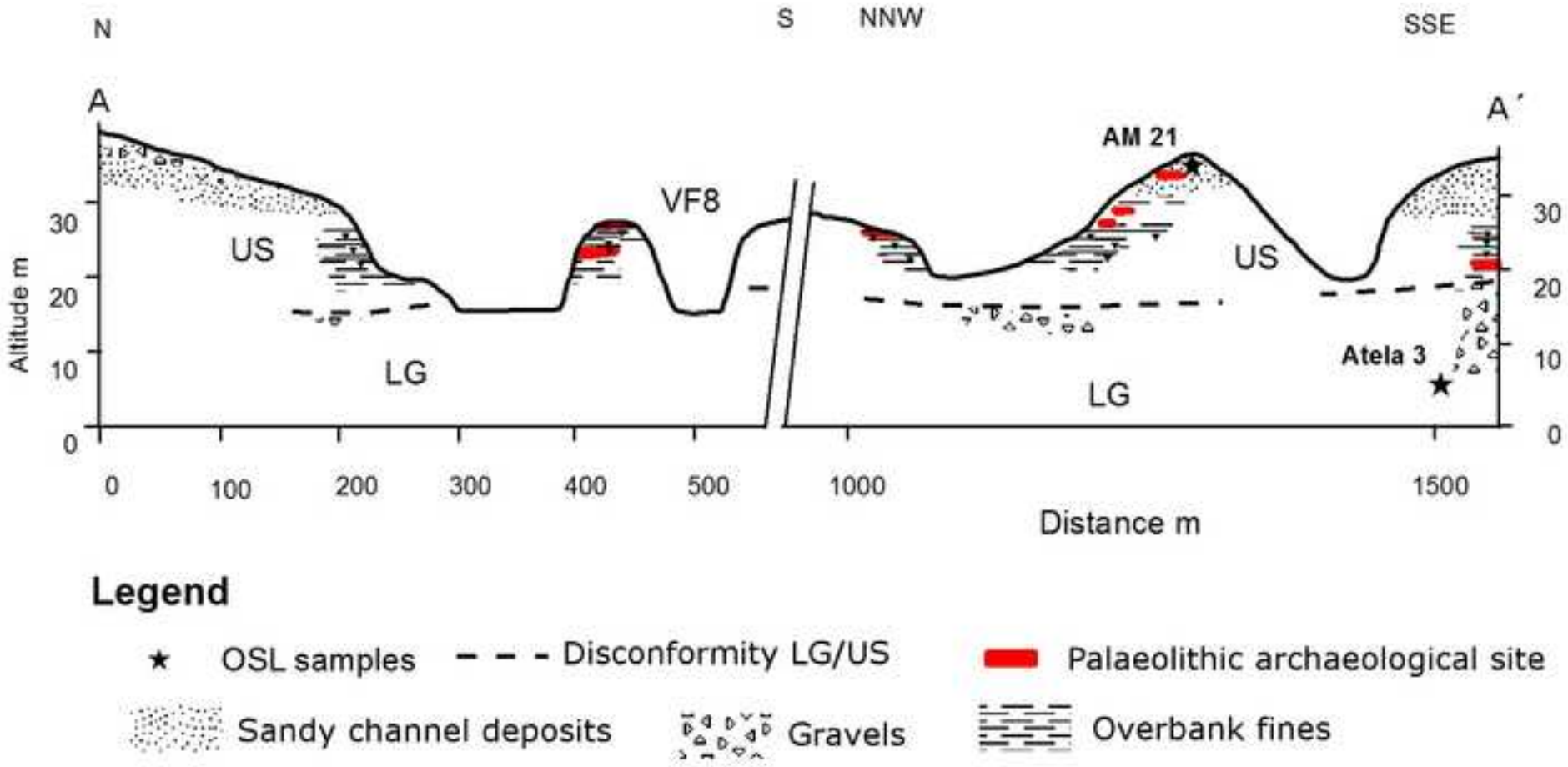

Figure6

Click here to download high resolution image

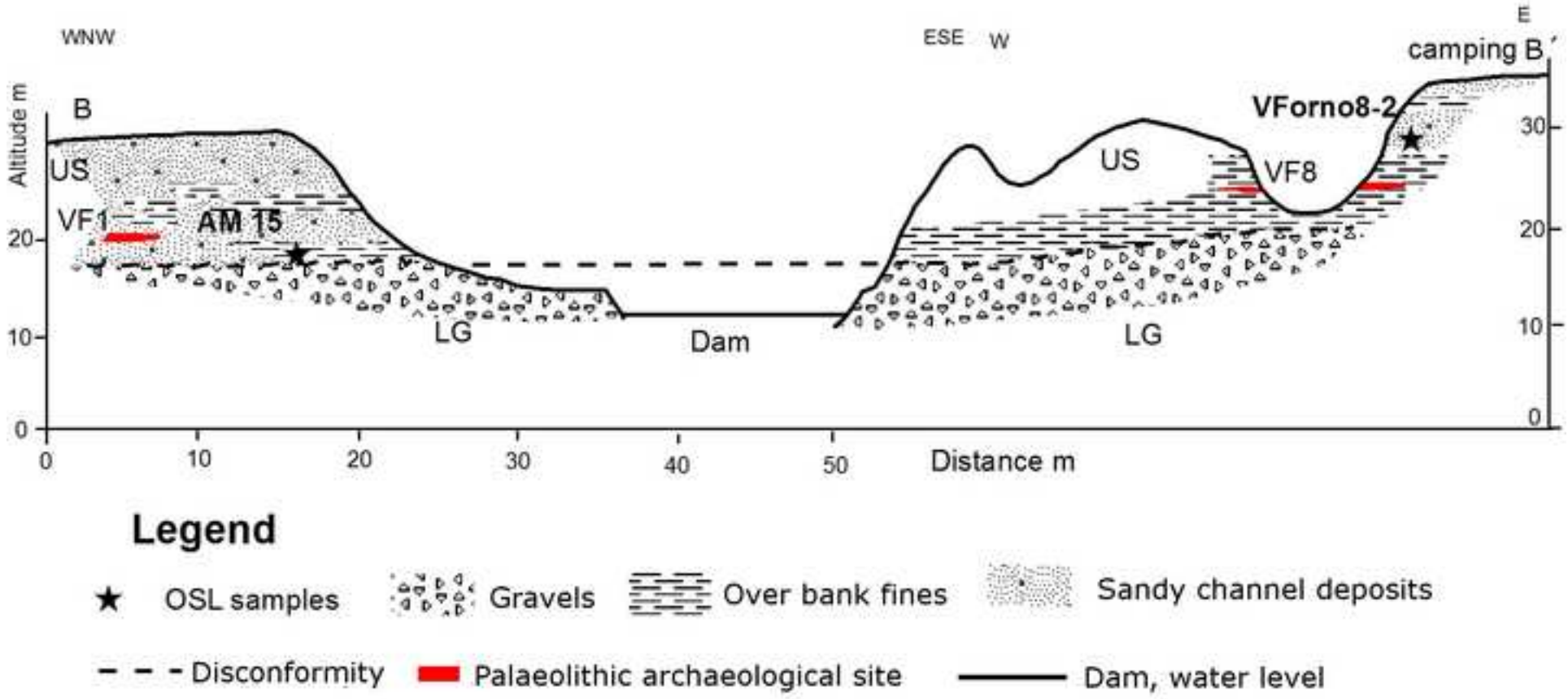

Figure7

Click here to download high resolution image

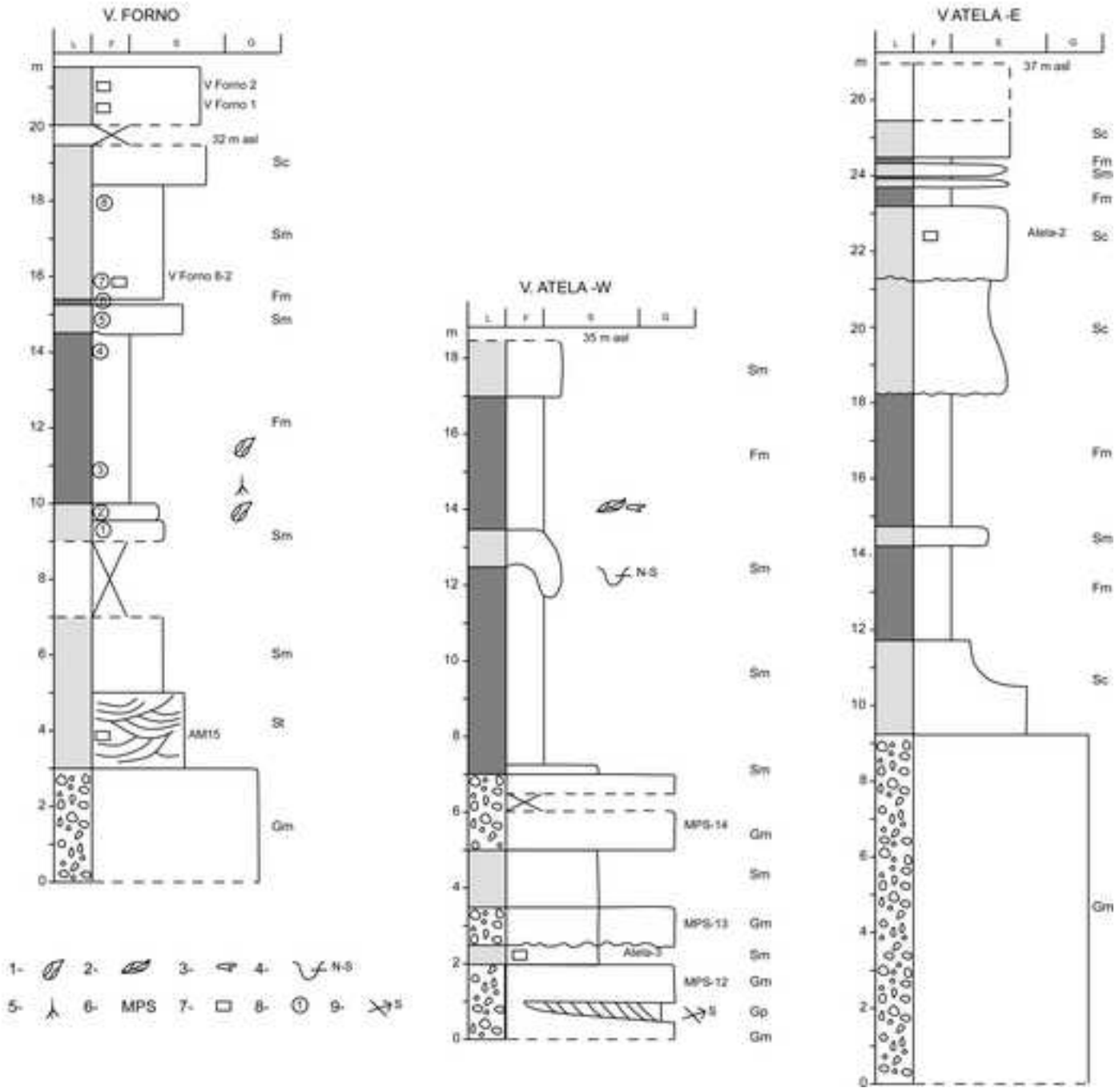

Figure8

Click here to download high resolution image

Figure9

Click here to download high resolution image

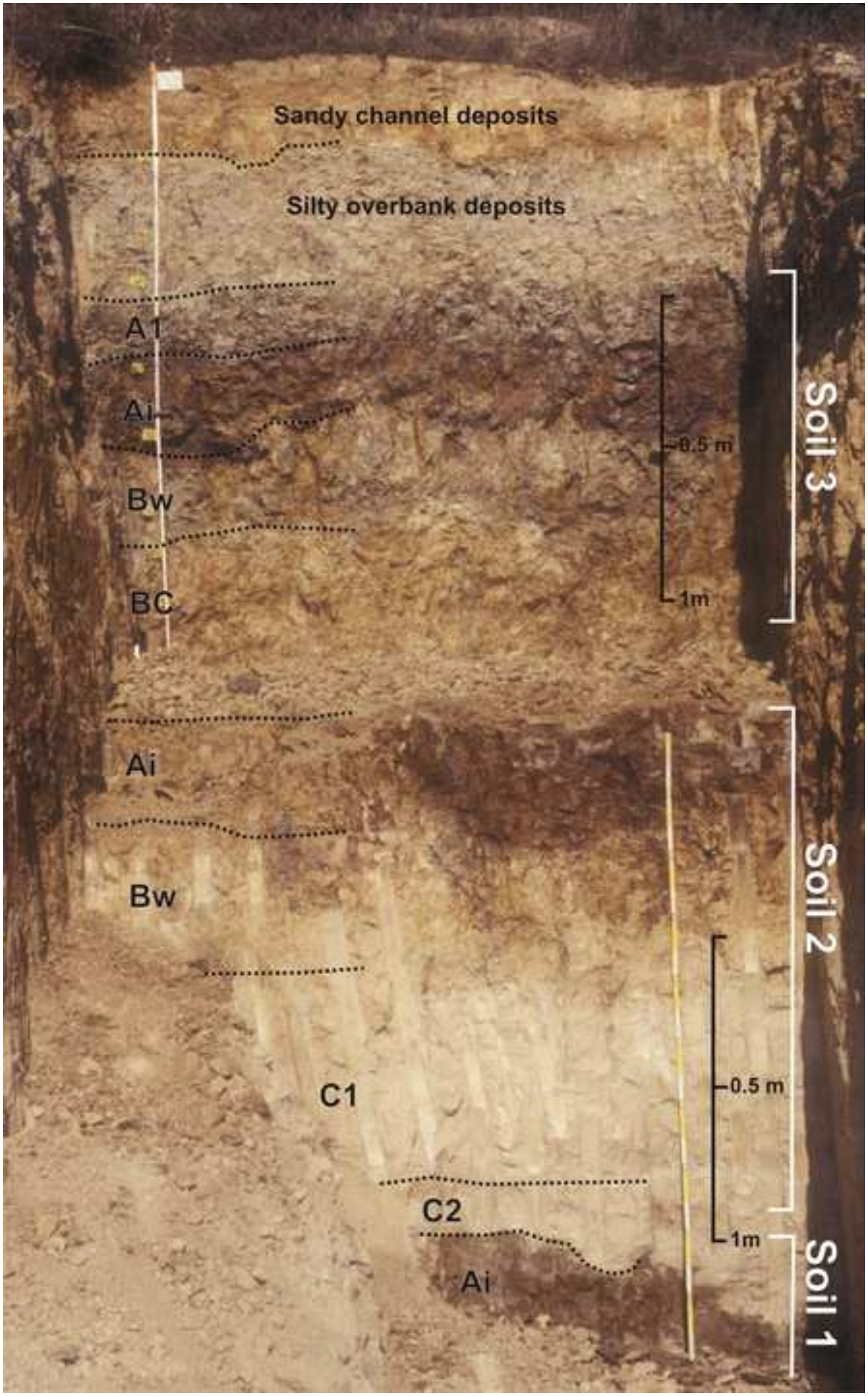

Figure10
Click here to download high resolution image

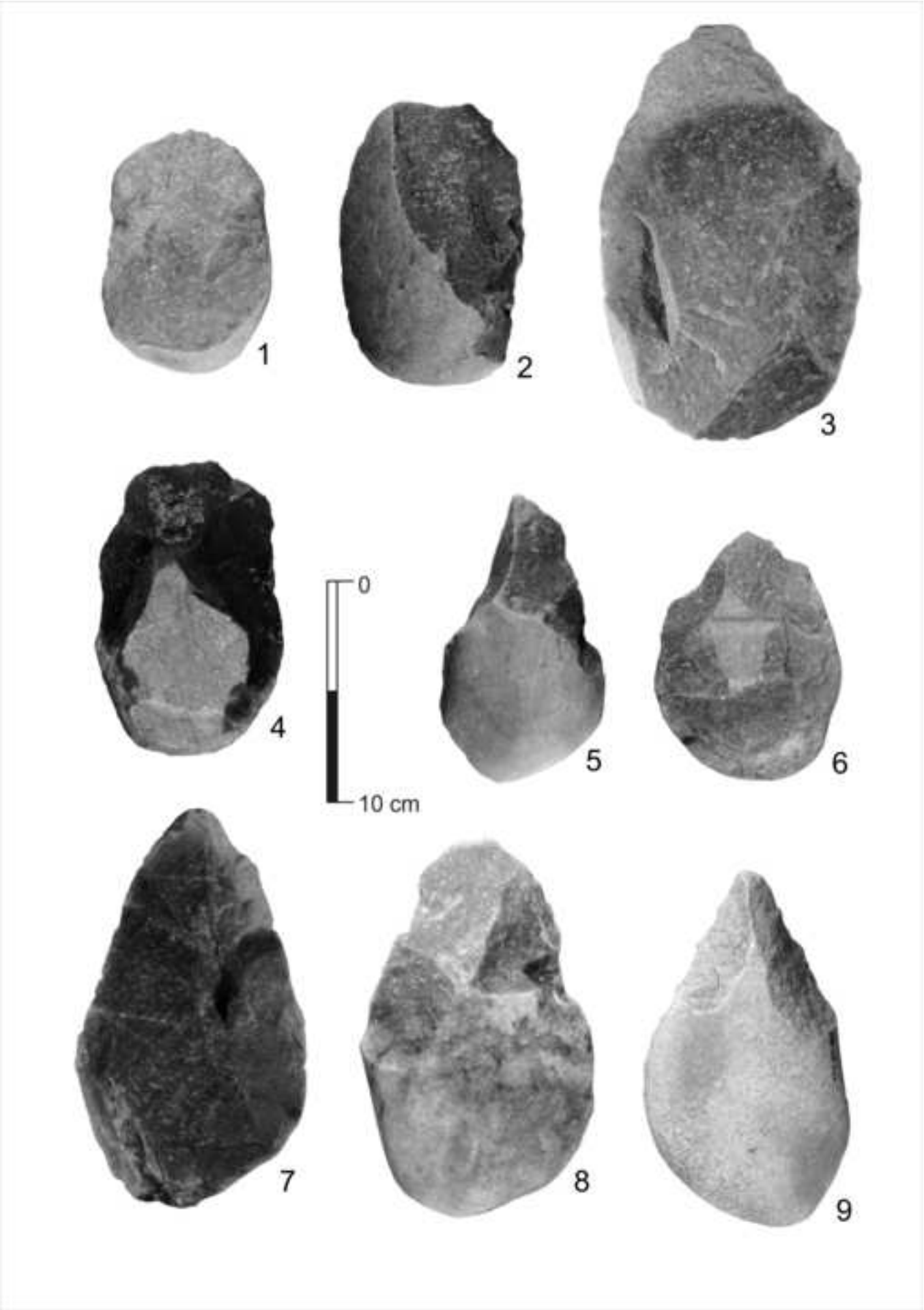

Figure11

Click here to download high resolution image

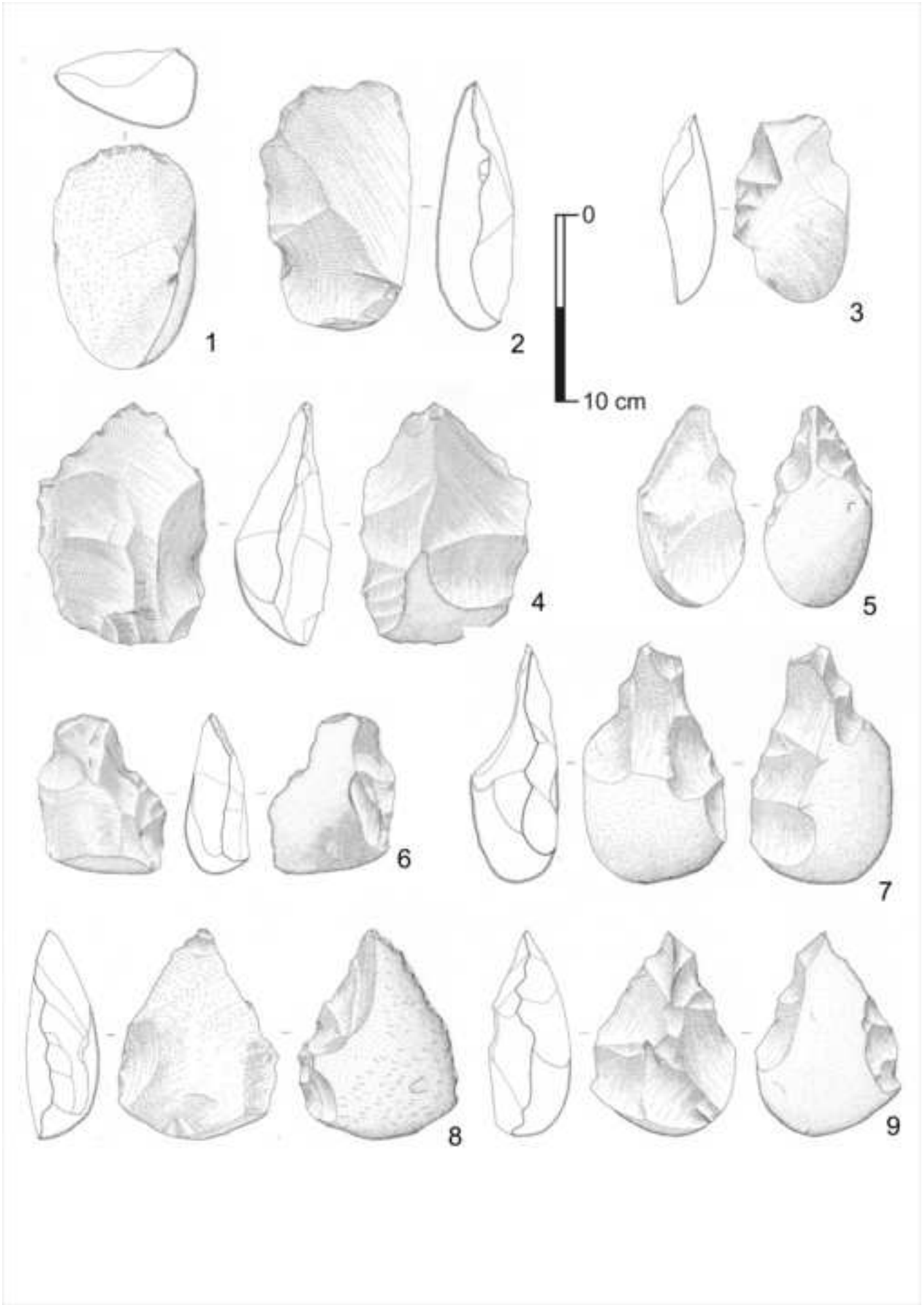

Figure12

Click here to download high resolution image

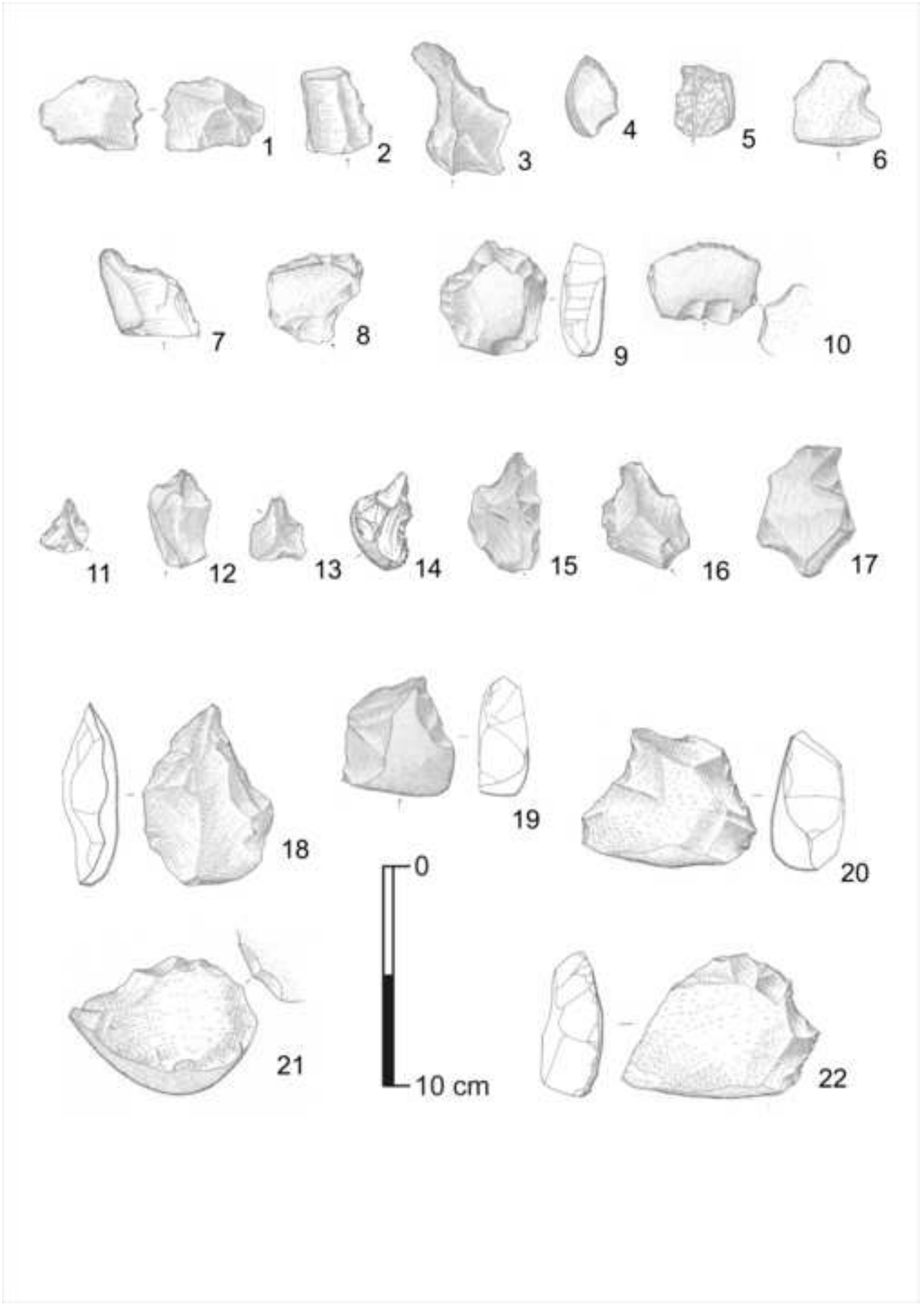

Figure13
Click here to download high resolution image

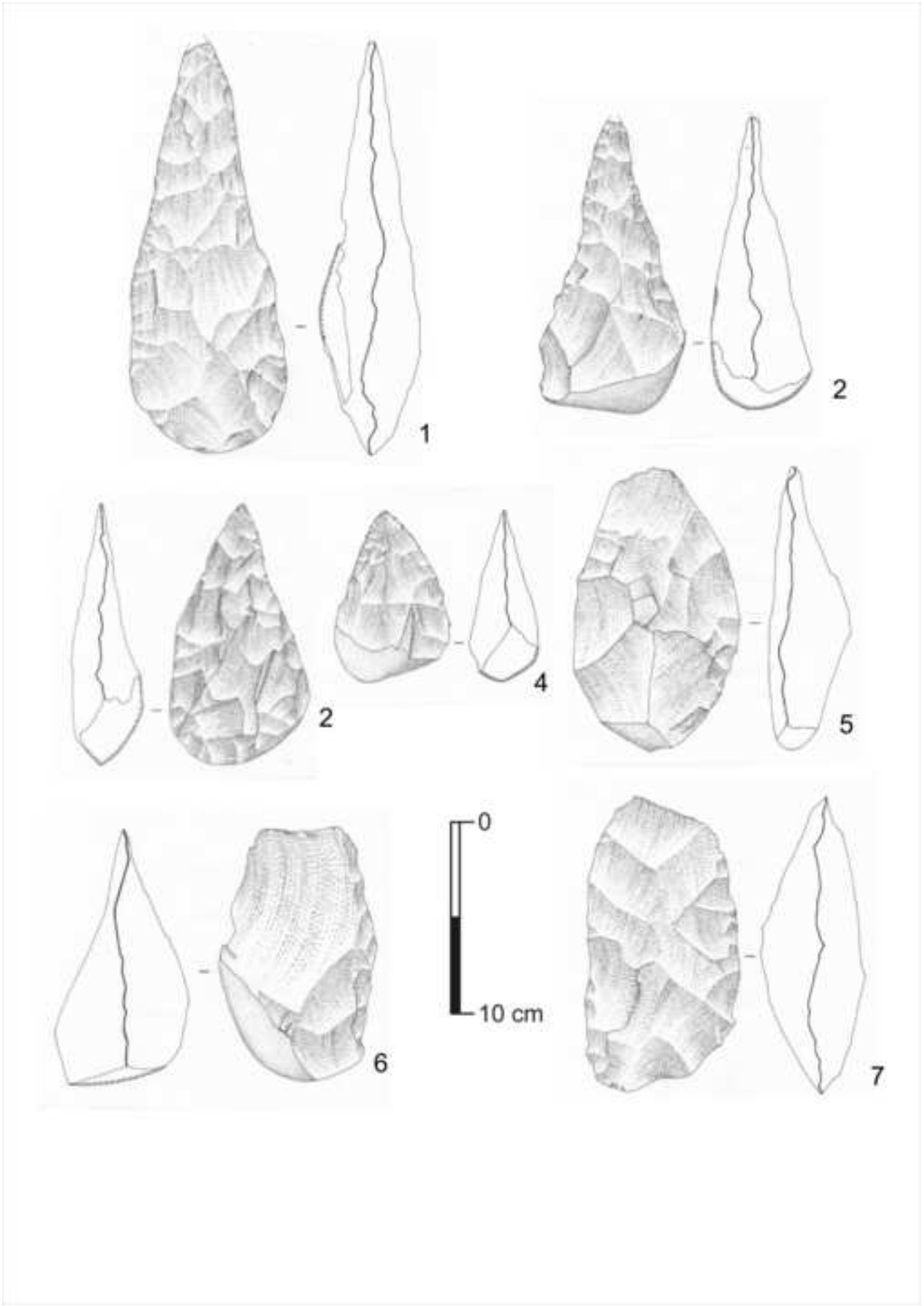

Figure14
Click here to download high resolution image

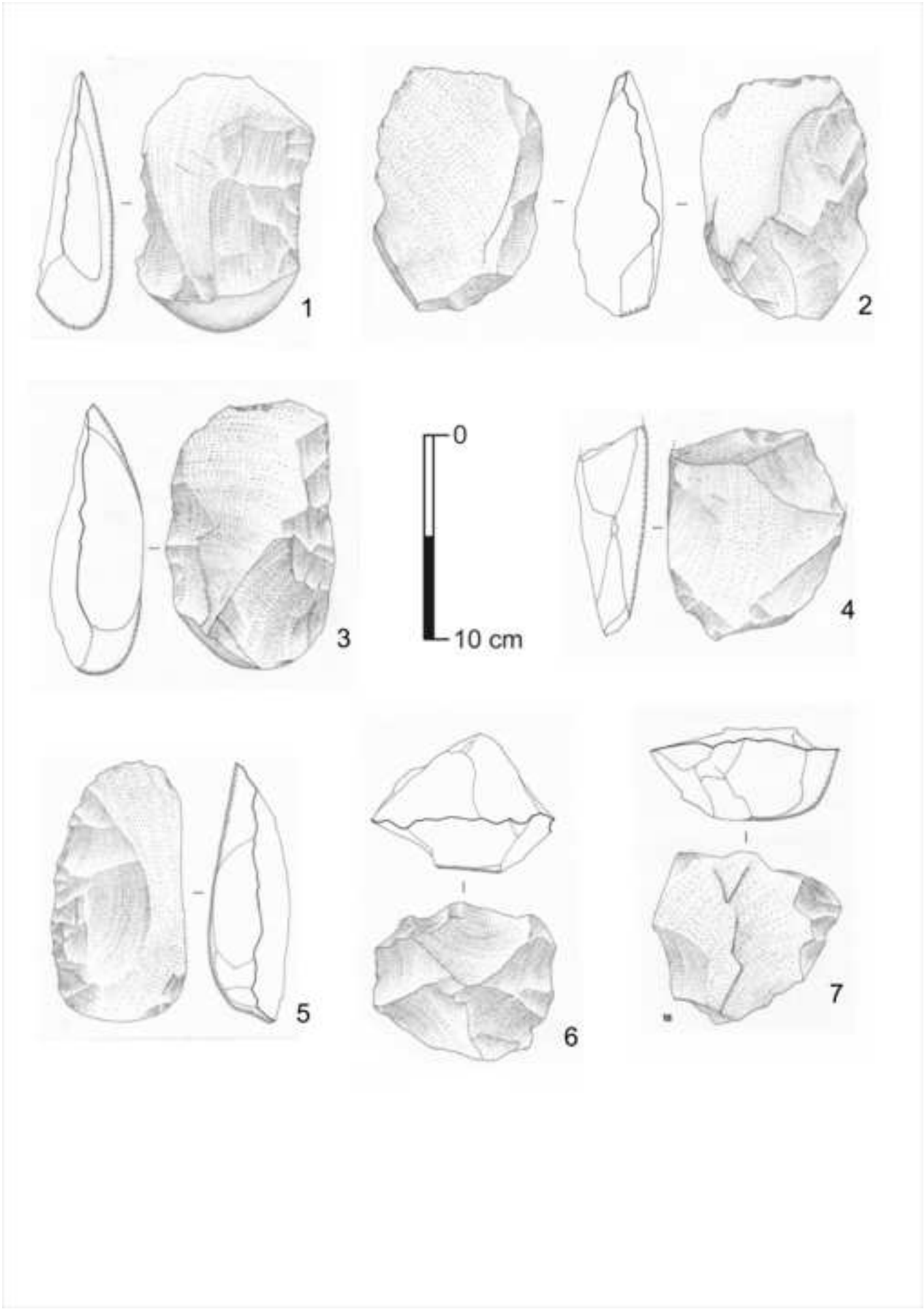

Figure15

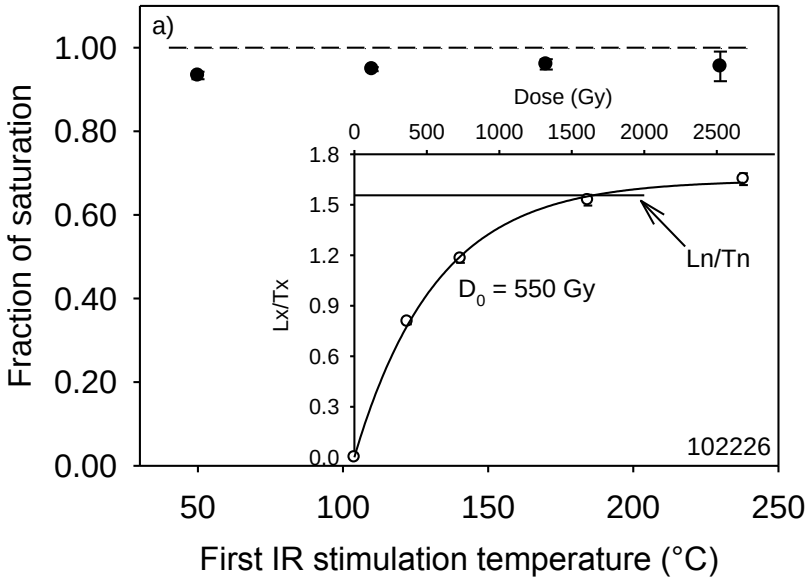
a)
Fraction of saturation
1.00
0.80
0.60
0.40
0.20
0.00
50
100
150
200
250
First IR stimulation temperature (°C)
Dose (Gy)
0
500
1000
1500
2000
2500
Lx/Tx
1.8
1.5
1.2
0.9
0.6
0.3
0.0
Ln/Tn
D0 = 550 Gy
102226

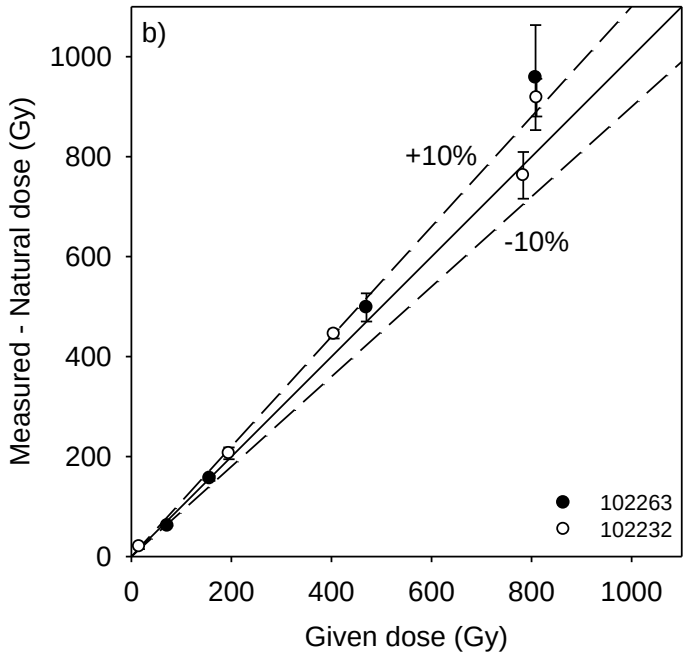
b)
Measured - Natural dose (Gy)
1000
800
600
400
200
0
+10%
-10%
102263
102232
0
200
400
600
800
1000
Given dose (Gy)

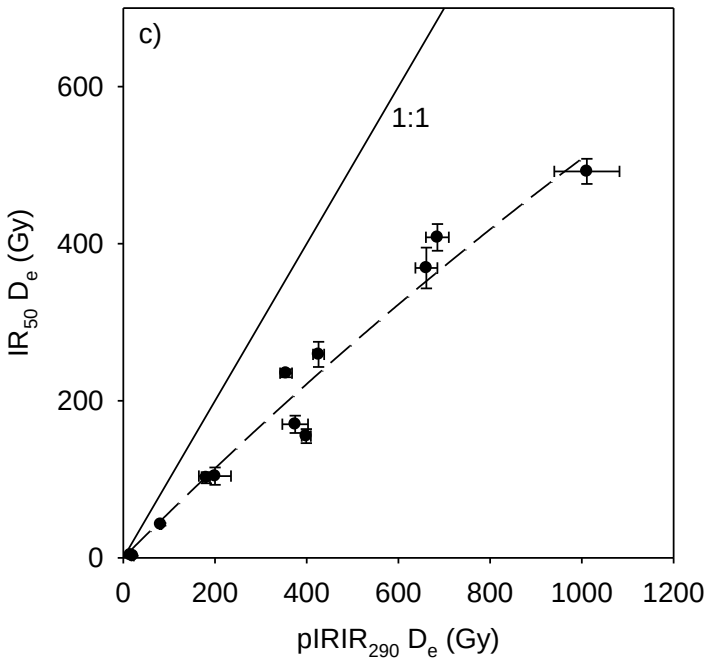
c)
IR50 De (Gy)
600
400
200
0
1:1
0
200
400
600
800
1000
1200
pIRIR290 De (Gy)

Figure16

Click here to download high resolution image

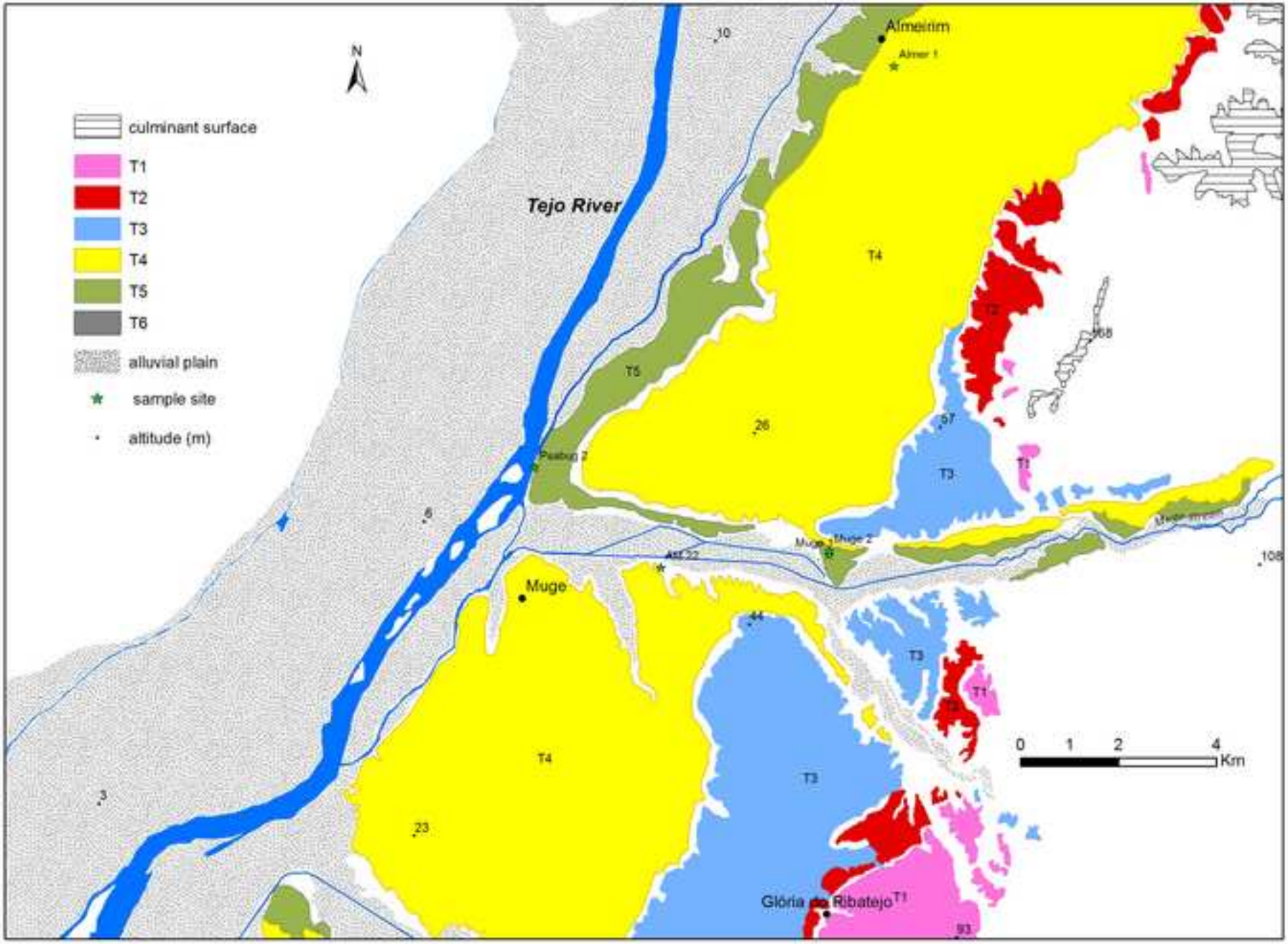

Figure17

Click here to download high resolution image